

FINAL Report B

TRyy1110

**Project Title: Design and Evaluation of High-Volume
Fly Ash (HVFA) Concrete Mixes**

**Report B: Bond Behavior of Mild Reinforcing Steel in
HVFA Concrete**

Prepared for
Missouri Department of Transportation
Construction and Materials

Missouri University of Science and Technology, Rolla, Missouri

October 2012

The opinions, findings, and conclusions expressed in this publication are those of the principal investigators and the Missouri Department of Transportation. They are not necessarily those of the U.S. Department of Transportation, Federal Highway Administration. This report does not constitute a standard or regulation.

ABSTRACT

The main objective of this study was to determine the effect on bond performance of high-volume fly ash (HVFA) concrete. The HVFA concrete test program consisted of comparing the bond performance of two concrete mix designs with 70% cement replacement with Class C fly ash relative to a Missouri Department of Transportation (MoDOT) standard mix design.

Two test methods were used for bond strength comparisons. The first was a direct pull-out test based on the RILEM 7-II-128 “RC6: Bond test for reinforcing steel. 1. Pull-out test” (RILEM, 1994). The direct pull-out tests were performed on specimens with #4 (#13) and #6 (#19) deformed reinforcing bars.

The second test method consisted of a full-scale beam splice test specimen subjected to a four-point loading until failure of the splice. This test method is a non-ASTM test procedure that is generally accepted as the most realistic test method for both development and splice length. The beam splice tests were performed on beams with #6 (#19) reinforcing bars spliced at midspan at a specific length to ensure bond failure occurred prior to shear or flexural failure.

Analysis of the HVFA concrete test data indicates that using greater than 50% replacement of cement with fly ash in concrete does not result in any increase in the required development length of mild reinforcing steel.

TABLE OF CONTENTS

	Page
ABSTRACT.....	ii
LIST OF ILLUSTRATIONS.....	vi
LIST OF TABLES.....	viii
NOMENCLATURE.....	ix
SECTION	
1. INTRODUCTION.....	1
1.1. BACKGROUND AND JUSTIFICATION FOR HIGH-VOLUME FLY ASH RESEARCH.....	1
1.1.1. General.....	1
1.1.2. Fly Ash.....	1
1.1.3. Benefits of High-Volume Fly Ash Concrete.....	2
1.1.4. Concerns with HVFA Concrete.....	2
1.2. OBJECTIVE & SCOPE OF WORK.....	3
1.3. RESEARCH PLAN.....	3
1.4. OUTLINE.....	4
2. LITERATURE REVIEW.....	5
2.1. BOND CHARACTERISTICS.....	5
2.2. COMMON BOND TESTS.....	8
2.3. COAL FLY ASH ORIGIN AND USES.....	11
2.4. HIGH-VOLUME FLY ASH CONCRETE BOND RESEARCH.....	14
3. MIX DESIGNS AND CONCRETE PROPERTIES.....	18
3.1. INTRODUCTION.....	18
3.2. CONCRETE PROPERTIES.....	18
3.2.1. Fresh Concrete Properties.....	18
3.2.2. Compressive Strength of Concrete.....	20
3.2.3. Modulus of Rupture of Concrete.....	22
3.2.4. Splitting Tensile Strength of Concrete.....	24
3.3. HIGH-VOLUME FLY ASH (HVFA) CONCRETE MIX DESIGNS.....	25

3.3.1. HVFA Control Mix Design and Concrete Properties	25
3.3.2. HVFA 70% Replacement, High Cementitious Material Mix Design and Concrete Properties	27
3.3.3. HVFA 70% Replacement, Low Cementitious Material Mix Design and Concrete Properties	30
4. EXPERIMENTAL PROGRAM.....	33
4.1. INTRODUCTION	33
4.2. DIRECT PULL-OUT TEST.....	33
4.2.1. Direct Pull-out Specimen Design	33
4.2.2. Direct Pull-out Specimen Fabrication	36
4.2.3. Direct Pull-out Test Setup	38
4.2.4. Direct Pull-out Test Procedure	39
4.3. BEAM SPLICE TEST	40
4.3.1. Beam Splice Specimen Design.....	40
4.3.2. Beam Splice Specimen Fabrication.....	42
4.3.3. Beam Splice Specimen Test Setup.....	48
4.3.4. Beam Splice Test Procedure.....	50
5. HVFA TEST RESULTS AND EVALUATION.....	51
5.1. DIRECT PULL-OUT TEST RESULTS.....	51
5.2. BEAM SPLICE TEST RESULTS.....	57
5.3. REINFORCING BAR TENSION TEST	64
5.4. ANALYSIS OF RESULTS	64
5.4.1. Methodology	64
5.4.2. Analysis and Interpretation – Direct Pull-out Test Results	67
5.4.3. Analysis and Interpretation – Beam Splice Test Results	71
5.5. FINDINGS AND CONCLUSIONS	77
6. FINDINGS, CONCLUSIONS, AND RECOMMENDATIONS	78
6.1. FINDINGS	78
6.1.1. Direct Pull-out Testing	78
6.1.2. Beam Splice Testing.....	79
6.2. CONCLUSIONS.....	79

6.2.1. Direct Pull-out Testing	79
6.2.2. Beam Splice Testing.....	80
6.3. RECOMMENDATIONS	80
APPENDICES	
A. HVFA TEST PROGRAM BEAM SPLICE FAILURE PHOTOGRAPHS	82
B. HVFA TEST PROGRAM TEST DATA PLOTS	92
C. HVFA TEST PROGRAM STATISTICAL ANALYSIS	100
BIBLIOGRAPHY.....	104

LIST OF ILLUSTRATIONS

Figure	Page
2.1. Stress transfer between steel and surrounding concrete (ACI 408R, 2003)	6
2.2. Direct pull-out test specimen (ACI 408R, 2003)	9
2.3. Beam-end pull-out test specimen (ACI 408R, 2003).....	10
2.4. Beam anchorage test specimen (ACI 408R, 2003).....	11
2.5. Beam splice test specimen (ACI 408R, 2003).....	11
3.1. Slump test.....	19
3.2. Casting compressive strength cylinders.....	21
3.3. Compressive strength test setup.....	21
3.4. Modulus of rupture test specimens	23
3.5. Modulus of rupture test setup	23
3.6. Splitting tensile strength test setup	24
3.7. Plot of HVFA-C compressive strength	26
3.8. Plot of HVFA-70H compressive strength.....	29
3.9. Plot of HVFA-70L compressive strength	31
4.1. Pull-out specimen with dimensions for #4 (#13) reinforcing bars	35
4.2. Pull-out specimen with dimensions for #6 (#19) reinforcing bars	35
4.3. Pull-out specimen construction.....	37
4.4. Completed specimens	38
4.5. Direct pull-out test setup.....	39
4.6. LVDT installation to measure bar slip.....	39
4.7. Beam splice specimen reinforcing layout	42
4.8. Beam splice specimen cross section	42
4.9. Finished reinforcing bar cage.....	44
4.10. Spliced longitudinal bars for normal strength concrete	45
4.11. Reinforcing bar cages in beam forms	45
4.12. Concrete bucket being filled with fresh concrete	46
4.13. Placement of concrete into beam forms.....	47
4.14. Finished beams in forms	47

4.15. Beam loading schematic	48
4.16. Beam positioned within load frame	49
4.17. LVDT installation	50
5.1. Adding calcium hydroxide to the mixing truck	52
5.2. HVFA-C pull-out test results	54
5.3. HVFA-70H pull-out test results.....	54
5.4. HVFA-70L pull-out test results	55
5.5. Example applied load vs. slip plot	56
5.6. HVFA-C6PO3 failed specimen	56
5.7. HVFA-C6PO3 applied load vs. slip plot	57
5.8. HVFA-C peak load plot	59
5.9. HVFA-70H peak load plot.....	60
5.10. HVFA-70L peak load plot	60
5.11. Typical load vs. deflection plot.....	61
5.12. Typical load vs. strain plot.....	62
5.13. Cracked length of HVFA-70HBB2	62
5.14. Failed splice region of HVFA-70HBB2	63
5.15. Bottom of splice region of HVFA-70HBB2.....	63
5.16. Plot of normalized average peak load for each HVFA concrete mix design.....	68
5.17. Normalized load vs. slip plot for #4 (#13) reinforcing bars	70
5.18. Load vs. slip plot for #6 (#19) reinforcing bars	70
5.19. Normalized peak load	73
5.20. Normalized steel stress at failure load	73
5.21. Typical normalized load vs. strain plot.....	76

LIST OF TABLES

Table	Page
2.1. Chemical composition requirements of fly ash (ASTM C618-12, 2012).....	13
2.2. Physical property requirements of fly ash (ASTM C618-12, 2012).....	13
3.1. HVFA-C mix proportions	26
3.2. Compressive strength data of HVFA-C.....	26
3.3. Splitting tensile strength test results for HVFA-C.....	27
3.4. Modulus of rupture test results for HVFA-C.....	27
3.5. HVFA-70H mix proportions.....	28
3.6. Compressive strength data of HVFA-70H.....	28
3.7. Splitting tensile strength test results for HVFA-70H.....	29
3.8. Modulus of rupture test results for HVFA-70H.....	30
3.9. HVFA-70L mix proportions	30
3.10. Compressive strength data of HVFA-70L	31
3.11. Splitting tensile strength test results for HVFA-70L	32
3.12. Modulus of rupture test results for HVFA-70L	32
5.1. HVFA concrete direct pull-out test matrix	51
5.2. HVFA concrete pull-out test results	53
5.3. HVFA concrete beam splice test matrix	58
5.4. Peak load and reinforcing bar stresses	59
5.5. #6 (#19) reinforcing bar tension test results	64
5.6. Test day compressive strengths for test specimens.....	67
5.7. Normalized HVFA concrete pull-out test results.....	69
5.8. Normalized peak loads for each specimen.....	72
5.9. Normalized steel stress at failure for each specimen	74
5.10. Normalized steel stress compared to theoretical steel stress at failure	75

NOMENCLATURE

Symbol	Description
A_b	Area of reinforcing bar
c	Spacing or cover dimension
c_b, c_{min}	Smaller of the distance from center of a bar to nearest concrete surface or one-half the center-to-center spacing of bars being developed
c_{max}	Larger of the distance from center of a bar to nearest concrete surface or one-half the center-to-center spacing of bars being developed
d_b	Nominal diameter of reinforcing bar
f'_c	Specified compression strength of concrete
f_y	Specified yield strength of reinforcement
K_{tr}	Transverse reinforcement index
l_d, l_{db}	Development length
α, ϕ_t	Reinforcement location modification factor
β, ϕ_e	Reinforcement coating modification factor
λ	Lightweight concrete modification factor
ω	$0.1 (c_{max}/c_{min}) + 0.9 \leq 1.25$
ϕ_s	Reinforcement size modification factor

1. INTRODUCTION

1.1. BACKGROUND AND JUSTIFICATION FOR HIGH-VOLUME FLY ASH RESEARCH

1.1.1. General. Concrete is the world's most consumed man-made material. Unfortunately, the production of portland cement, the active ingredient in concrete, generates a significant amount of carbon dioxide. For each pound of cement produced, approximately one pound of carbon dioxide is released into the atmosphere. With cement production reaching nearly 6 billion tons per year worldwide, the sustainability of concrete is a very real concern. Since the 1930's, fly ash – a pozzolanic material – has been used as a partial replacement of portland cement in concrete to improve the material's strength and durability, while also limiting the amount of early heat generation (Volz and Myers, 2011).

1.1.2. Fly Ash. Fly ash is a siliceous material that has the capacity to create cementitious compounds when combined with water. However, due to differences in coals from different sources and designs of coal-fired boilers, not all fly ash produced is similar in composition. The chemical composition of fly ash could differ depending on where it was produced and by which company. Due to this variation in composition, standards were created to regulate the composition of fly ash used for specific purposes. For example, fly ash meant to be used as a replacement of portland cement in concrete must meet requirements set in ASTM C618-12, "Standard Specification for Coal Fly Ash and Raw or Calcined Natural Pozzolan for Use in Concrete." ASMT C618-12 defines two classes of fly ash, Class F and Class C, which are acceptable for use in concrete.

Class F fly ash is produced from the combustion of anthracite or bituminous coal and exhibits only pozzolanic properties. Class C fly ash is produced from the combustion of lignite or subbituminous coals and exhibits pozzolanic and cementitious properties (Federal Highway Administration, 2011).

1.1.3. Benefits of High-Volume Fly Ash Concrete. From an environmental perspective, replacing cement with fly ash reduces concrete's overall carbon footprint and diverts an industrial by-product from the solid waste stream. Traditional specifications limit the amount of fly ash to 25 or 30% cement replacement. Recent studies have shown that higher cement replacement percentages – even up to 70 % – can result in excellent concrete in terms of both strength (Wolfe, 2011) and durability (Marlay, 2011). Referred to as high-volume fly ash (HVFA) concrete, this material offers a viable alternative to traditional portland cement concrete and is significantly more sustainable (Volz and Myers, 2011).

1.1.4. Concerns with HVFA Concrete. At all replacement rates, fly ash generally slows down the setting time and hardening rates of concrete at early ages, especially under cold weather conditions, and when less reactive fly ashes are used. Furthermore, with industrial by-products, some variability in physical and chemical characteristics will normally occur, not only between power plants, but also within the same plant. Consequently, to achieve the benefits of HVFA concrete, guidelines are needed for its proper application in bridges, roadways, culverts, retaining walls, and other transportation-related infrastructure components (Volz and Myers, 2011).

1.2. OBJECTIVES & SCOPE OF WORK

The main objective of this study was to determine the effect on bond performance of HVFA concrete. The HVFA concrete test program consisted of comparing the bond performance of two concrete mix designs with 70% cement replacement with Class C fly ash relative to a Missouri Department of Transportation (MoDOT) standard mix design at one strength level.

The following scope of work was implemented in an effort to attain these objectives: (1) review applicable literature; (2) develop a research plan; (3) design and construct test fixtures; (4) design and construct test specimens; (5) test specimens to failure and record applicable data; (6) analyze results and conduct comparisons between experimental and control mix designs; (7) develop conclusions and recommendations; (8) prepare this report in order to document the information obtained during this study.

1.3. RESEARCH PLAN

The research plan entailed determining the bond performance of HVFA concrete relative to MoDOT standard mix designs. For the HVFA concrete test program, two concrete mix designs with 70% replacement of cement with Class C fly ash, one with a relatively high cementitious material content and the other with a relative low cementitious material content, were used for comparison.

Two test methods were used for bond strength comparisons. The first was a direct pull-out test based on the RILEM 7-II-128 “RC6: Bond test for reinforcing steel. 1. Pull-out test” (RILEM, 1994). Although not directly related to the behavior of a reinforced concrete beam in flexure, the test does provide a realistic comparison of bond between

types of concrete. A total of 18 direct pull-out test specimens were constructed and tested to bond failure using this test method. The second test method consisted of a full-scale beam splice test specimen subjected to a four-point loading until failure of the splice. This test method is a non-ASTM test procedure that is generally accepted as the most realistic test method for both development and splice length. A total of 9 full-scale beam splice test specimens were constructed and tested to failure.

1.4. OUTLINE

This report consists of seven sections and six appendices. Section 1 briefly explains the characteristics, benefits, and concerns of HVFA concrete, as well as the study's objective and the manner in which the objective was attained.

Section 2 explains the mechanisms behind bond strength of deformed reinforcing bars embedded in concrete, common methods for testing bond strength, coal fly ash origins and uses, and past bond research conducted on HVFA concrete.

Section 3 details the mix designs used in this study and their associated fresh concrete properties as well as the mechanical and strength properties determined at the time of bond testing.

Section 4 details the direct pull-out and beam splice test specimen design, fabrication, and testing setup and procedure.

Sections 5 the test result normalization process, the recorded test program results, normalized test results, and the comparisons of HVFA concrete the control mix design.

Section 7 restates the findings that were established during the course of this study and presents conclusions and recommendations based on the test results obtained.

2. LITERATURE REVIEW

2.1. BOND CHARACTERISTICS

Due to its very low tensile strength, concrete, by itself, would be a poor structural material to use in members resisting anything but a concentric axial compressive load. The tensile strength of concrete is generally only 10% of its compressive strength. However, the addition of steel reinforcing bars in the areas of the cross section of the member experiencing tensile stresses has proven to be a suitable solution to overcoming the poor tensile strength of concrete. The high tensile strength of steel is able to withstand the tensile stresses upon failure of the concrete. In order to obtain complete composite behavior between the reinforcing steel and the concrete, the tensile stresses must be fully transferred to the steel from the concrete. This transfer of stresses is facilitated by an adequate bond between the steel reinforcing bars and concrete.

The three modes of stress transfer from concrete to deformed steel reinforcement are through chemical adhesion, friction along the steel-concrete interface, and bearing resistance of the ribs on the steel against the surrounding concrete, as shown in **Figure 2.1**. Chemical adhesion refers to the bonding of the steel to the concrete through chemical reactions between the two surfaces. Upon initial loading, the resistance through chemical adhesion is the first stress transfer mechanism to fail. Upon failure of the chemical adhesion, the slipping action of the bar initiates the transfer of stresses from friction and rib anchorage. Frictional forces developed along the smooth faces of the reinforcing bar are relatively small compared to the forces transferred through the ribs. As the bar slip

increases, stress transfer through friction decreases, to a point where most of the tensile stresses are transferred through anchorage of the ribs.

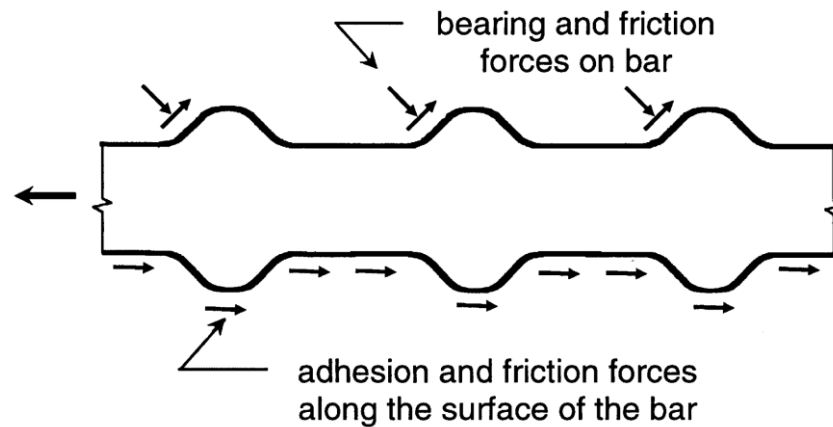


Figure 2.1 – Stress transfer between steel and surrounding concrete (ACI 408R, 2003)

As the load is increased, complete failure of the bond will occur by the concrete crushing against the ribs. One type of bond failure results when the bar is pulled directly out of the concrete, creating a shear plane along the outer edges of the steel ribs. This occurs when there is sufficient concrete cover and clear spacing between the reinforcing bars. Another type of bond failure is a splitting failure of the concrete cover. This occurs when there is insufficient concrete cover or insufficient clear spacing between the reinforcing bars (ACI 408R, 2003).

With adequate bond, tensile stresses can be transferred from the concrete to the reinforcing bar such that the bar will fail through yielding, and eventually fracture. The shortest length required to increase the stress of the bar from zero to the yield stress is called the development length of the bar. The development length of reinforcing steel is dependent on the bar diameter and yield stress, as well as the coefficient of friction on the

steel/concrete interface. The need for reinforcement splices is common in monolithic construction of large members, such as columns extending multiple levels of a structure. The allowable types of tension splices are lapped splices, mechanical splices, and welded splices. Lap splices are the transfer of tensile stresses from one bar to the concrete, then from the concrete to another bar by overlapping the two reinforcing bars. The overlapping distance must be at least the development length of the bar. Mechanical splices are achieved through the use of various steel devices that connect the ends of the two bars being spliced. Welded splices consist of welding the two bars being spliced together (Wight and MacGregor, 2009).

The factors affecting the bond strength between reinforcing steel bars and concrete are a function of the structural characteristics of the member, as well as characteristics of the bar and concrete. One structural characteristic that plays a large role in affecting the bond strength of steel and concrete is the concrete cover and spacing between bars. As the concrete cover and bar spacing increase, the bond strength will also increase. The increase in bond strength is attributed to the decreasing likelihood of splitting failures with large spacing and cover. Another structural characteristic affecting bond strength is the presence of transverse reinforcement. The presence of transverse reinforcement surrounding the embedded bar slows the progressions of splitting cracks, which effectively increases bond strength. Also, the location of the bar during casting of the member affects the bond strength between the steel and concrete. Bars with a large volume of concrete cast below them have lower bond strengths than bars cast at the bottom of a member. This lower bond strength is caused by concrete settlement and the presence of excess bleed water around top-cast bars (ACI 408R, 2003).

Reinforcing bar and concrete properties also play a role in affecting the bond strength of steel and concrete. Bar size and geometry can greatly alter bond strength. Larger bars with higher relative rib areas achieve higher total bond forces than small bars. Bar surface condition, such as cleanliness and coating, significantly affect bond strength. While bars with rust and mill scale do not adversely affect bond strength, surface contaminants such as mud, oil, and other nonmetallic coatings will decrease bond strength. Also, epoxy coated bars have a tendency to reduce bond strength. Concrete properties such as compressive and tensile strength, and fracture energy will also affect bond strength. Increasing compressive and tensile strengths, and fracture energy will subsequently increase bond strength. The addition of transverse reinforcement also increases the extent that the concrete compressive strength affects bond strength. Also, increasing the aggregate percentage in a concrete mix, as well as aggregate strength, will increase bond strength (ACI 408R, 2003).

2.2. COMMON BOND TESTS

There have been numerous test methods created to determine the bond strength between concrete and steel reinforcing bars. There are four common methods of bond testing. Two small-scale test methods are the direct pull-out test and the beam-end pullout test. Two large-scale test methods are the beam anchorage test and the beam splice test. The direct pull-out test specimen, shown in **Figure 2.2**, is the most common of the four tests listed above due to the ease of fabricating the test specimens and performing the test. This test is run by supporting the concrete and applying tension to the reinforcing bar

until failure, as shown in **Figure 2.2**. This bond test is the least accurate test for defining the actual bond strength and is best used for comparison purposes only.

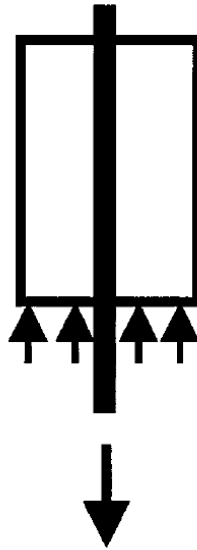


Figure 2.2 – Direct pull-out test specimen (ACI 408R, 2003)

The beam-end pull-out, also called the modified cantilever beam, test specimen is shown in **Figure 2.3**. This test is relatively easy to construct and perform and gives an accurate representation of how embedded reinforcing bars would behave in a full-scale beam. The compressive force applied must be located at least the same distance as the embedded length away from the end of the reinforcing bar. A length of reinforcing bar at the contact surface is left unbounded in order to prevent a conical failure surface from forming.

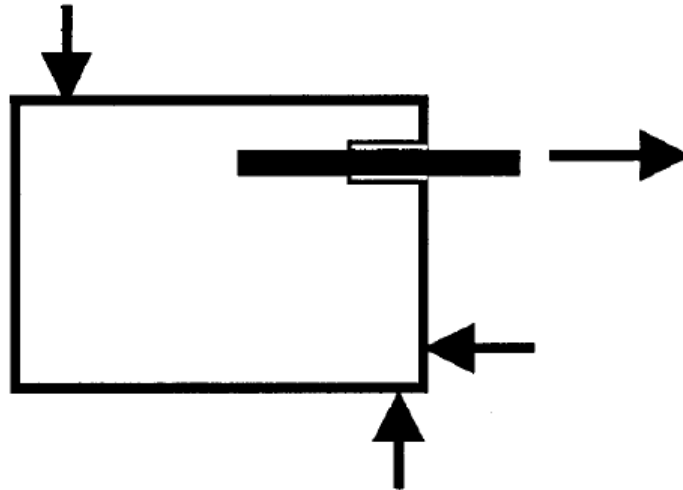


Figure 2.3 – Beam-end pull-out test specimen (ACI 408R, 2003)

The beam anchorage test specimen is shown in **Figure 2.4**. This test specimen is meant to represent a full-scale beam with a two cracked sections and a known length of bonded area. This test specimen is designed to measure development length of the reinforcing bar. **Figure 2.5** shows the beam splice test specimen. This test specimen is designed to measure the splice length of the reinforcing bar. The reinforcing bar splice placement and loading configuration is developed to subject the spliced region to a constant moment along the length of the splice. Current ACI 318-08 (ACI 318-08, 2008) design provisions for development length and splice length are based primarily on data from this type of test. Bond strengths determined from both test specimens are generally similar.

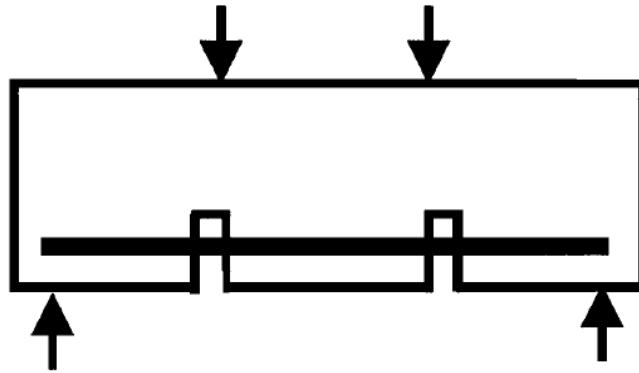


Figure 2.4 – Beam anchorage test specimen (ACI 408R, 2003)

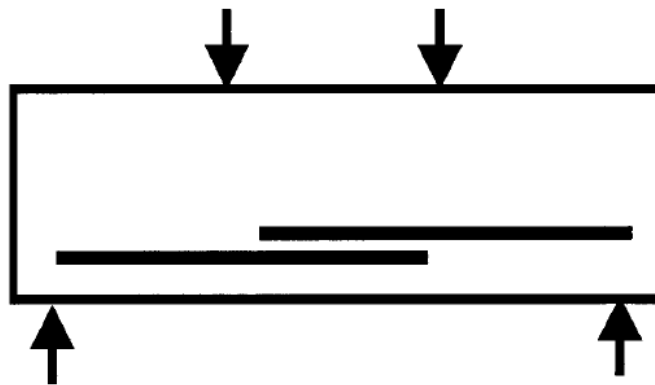


Figure 2.5 – Beam splice test specimen (ACI 408R, 2003)

2.3. COAL FLY ASH ORIGIN AND USES

Coal fly ash is one byproduct from the combustion of coal. The fly ash is a fine-grained, powdery particulate material that floats up the smoke stacks of typical electric producing facilities in flue gas. Current Environmental Protection Agency regulations require that the fly ash be collected before the combustion emissions are permitted to be released. Fly ash is usually collected from the flue gas by means of electrostatic precipitators, baghouses, or mechanical collection devices such as cyclones (Federal Highway Administration, 2011).

Fly ash is a versatile material with various potential applications due to its pozzolanic nature. It has been used as a substitute mineral filler in asphalt paving mixtures. Due to its chemical composition and fineness, fly ash generally meets the gradation, physical, and chemical requirements of mineral filler specifications. Fly ash can also be used as a fill or embankment material. Once compacted, fly ash at its optimum moisture content behaves similar to a well-compacted soil. Another beneficial use of fly ash is as a flowable fill, used as a substitute for compacted earth backfill. Depending on the pozzolanic properties of the specific fly ash, it can act as a fine aggregate, or as a cementitious material. No special processing of the fly ash is necessary for this application (Federal Highway Administration, 2011).

The single largest application of fly ash is as a replacement for portland cement in concrete. It is a siliceous material that has the capacity to create cementitious compounds when combined with water. However, due to differences in coals from different sources and designs of coal-fired boilers, not all fly ash produced is similar in composition. The chemical composition of fly ash could differ depending on where it was produced and by which company. Due to this variation in composition, standards were created to regulate the composition of fly ash used for specific purposes. For example, fly ash meant to be used as a replacement of portland cement in concrete must meet requirements set in ASTM C618-12, "Standard Specification for Coal Fly Ash and Raw or Calcined Natural Pozzolan for Use in Concrete." ASMT C618-12 defines two classes of fly ash, Class F and Class C, which are acceptable for used in concrete. Class F fly ash is produced from the combustion of anthracite or bituminous coal and exhibits only pozzolanic properties. Class C fly ash is produced from the combustion of lignite or subbituminous coals and

exhibits pozzolanic and cementitious properties (Federal Highway Administration, 2011).

Both classes of fly ash must conform to specific chemical compositions and physical properties as shown in **Table 2.1** and **2.2**, respectively (ASTM C618-12, 2012).

Table 2.1 – Chemical composition requirements of fly ash (ASTM C618-12, 2012)

	Class F	Class C
SiO₂, plus Al₂O₃, plus Fe₂O₃ min.	70%	50%
SO₃ max.	5%	5%
Moisture content	3%	3%
Loss of ignition	6%	6%

Table 2.2 – Physical property requirements of fly ash (ASTM C618-12, 2012)

		Class F	Class C
Fineness:	Amount retained when wet-sieved on No. 325 (45 µm) sieve, max	34%	34%
Strength activity index:	With portland cement, at 7 days, min, percent of control	75%	75%
	With portland cement, at 28 days, min, percent of control	75%	75%
	Water requirement, max, percent of control	105%	105%
Soundness:	Autoclave expansion or contraction, max	0.8%	0.8%
Uniformity requirements:	Density, max variation from average	5%	5%
	Percent retained on No. 325 (45 µm), max variation from average	5%	5%

2.4. HIGH-VOLUME FLY ASH CONCRETE BOND RESEARCH

High-volume fly ash (HVFA) concrete differs from conventional concrete in that a large amount of portland cement is replaced with fly ash, generally 50% or more. Current standards limit the amount of fly ash replacement in concrete to a maximum of 35%. Fly ash is a pozzolan and reacts with the excess calcium hydroxide that is the byproduct of the cement hydration process (Headwaters Resources, 2011). However, activators such as gypsum and calcium hydroxide are necessary to accelerate the development of the binder calcium silicate hydrate. Gypsum is added in order to accelerate the onset of early-age strength gain. Calcium hydroxide is added to supplement what is released by cement hydration to better develop long term strength gain.

Various studies have been conducted to analyze the effect of large fly ash replacement of cement in conventional concrete mixes. However, very few studies focus on the bond characteristics of HVFA concrete. One of the first investigations focusing on the bond strength of fly ash concrete with 10, 20, and 30% replacement of cement with fly ash was conducted at the Center for By-Products Utilization in 1989 and was entitled “Concrete Compressive Strength, Shrinkage, and Bond Strength as Affected by Addition of Fly Ash and Temperature.” The direct pull-out test specimens in this study were 6 in. (150 mm) diameter, 6 in. (150 mm) tall cylindrical concrete specimens with one reinforcing bar set vertically in the center. Each mix design was cured at a temperature of 73, 95, and 120 degrees Fahrenheit by keeping the specimens in temperature controlled rooms. The test results show that the ultimate bond stress increased with the addition of fly ash to a specific limit, and then decreased. The optimum fly ash replacement level

increased with the increase in testing temperature. The overall optimum fly ash replacement for cement was found to be 10 to 20% in this study (Naik *et al.*, 1989).

Another study focused on assessing the bond strength of HVFA concrete and was entitled “Structural Applications of 100 Percent Fly Ash Concrete” conducted at Montana State University (n.d.). The researchers conducted a series of direct pull-out tests for this study. The pull-out specimen consisted of a length of #4 (#13) reinforcing bar embedded at various lengths in 6 in. (152 mm) diameter, 12 in. (305 mm) tall cylinders of concrete. Six specimens were constructed for the conventional concrete mix design, as well as the 100% fly ash concrete mix design. Of those six specimens, the reinforcing bar was embedded 12 in. (305 mm) for three specimens, and 8 in. (203 mm) for the other three specimens. All the specimens were tested to failure. Failure for all the tested specimens consisted of splitting of the concrete section. This study indicated that the high-volume fly ash concrete mix had similar behavior as the conventional concrete mix (Cross, *et al.*, n.d.).

Another study on the bond strength of high-volume fly ash concrete was conducted at the Structural Engineering Research Centre in India and is entitled “Demonstration of Utilizing High Volume Fly Ash Based Concrete for Structural Applications” (2005). This study focused on determining the bond strength of a concrete mix design with 50% replacement of cement with fly ash. The researchers conducted a series of direct pull-out tests for this study. The test specimens consisted of a length of 0.79 in (20 mm) mild steel bars embedded in 5.9 in. (150 mm) concrete cubes. The results of the direct pull-out tests indicated that the high-volume fly ash concrete mix design exhibited the same level of bond strength as the conventional concrete mix design

at 28 and 56 days, and higher bond strength at 90 days. Also, the load vs. slip plot indicates both concrete mix designs exhibited similar behavior (Gopalakrishnan, 2005). This study highlights the advantage of high-volume fly ash concrete in terms of later age bond strength.

Most recently, a study was conducted at the Missouri University of Science and Technology to determine the bond performance of concrete with 70% replacement of cement with Class C fly ash relative to conventional concrete and was entitled “Bond Strength of High-Volume Fly Ash Concrete” (Wolfe, 2011). This study focused on comparing bond strengths of deformed reinforcing bar in both direct pull-out test specimens, as well as full-scale beam splice specimens. The direct pull-out specimens were based on the RILEM 7-II-128 “RC6: Bond test for reinforcing steel. 1. Pull-out test” (RILEM, 1994). A length of #4 (#13) and #6 (#19) deformed reinforcing bars were embedded in a 12 in. (305 mm) diameter concrete cylinder. The bars were embedded 10 times the bar diameter into the concrete section, with half of the embedded length debonded using a polyvinyl chloride (PVC) sleeve. There were six specimens tested for each bar size, with three for the conventional concrete mix design and three for the HVFA concrete mix design. All direct pull-out specimens were tested to pull-out failure. The beam splice specimens were 14 ft. (4270 mm) in length, with a cross section of 12 in. x 18 in. (305 mm x 457 mm). The longitudinal reinforcement consisted of three #6 (#19) reinforcing bars that were spliced at midspan a length of 16.55 in. (420 mm). The beams were subjected to four-point loading to ensure the splice region was subjected to constant moment along its length. For beam specimens without confinement, the transverse reinforcement consisted of #3 (#10) closed stirrups spaced at 7 in. (178 mm) up until the

splice on either side. For beam specimens with confinement, the transverse reinforcement consisted of #3 (#10) closed stirrups spaced at 7 in. (178 mm) along the entire length of the beam. Six beams were tested for each mix design, of which three contained a confined splice and three an unconfined splice. All beam splice specimens were tested to failure of the splice. The author concluded that 70% replacement of cement with Class C fly ash is not only feasible in terms of bond, but is superior in some cases (Wolfe, 2011).

3. MIX DESIGNS AND CONCRETE PROPERTIES

3.1. INTRODUCTION

The following chapter contains the mix designs for the high-volume fly ash (HVFA) concretes evaluated in this study, as well as the control mix design used for comparison. Also included in this chapter are the methods and results of the testing done to determine the fresh and hardened properties of each mix.

3.2. CONCRETE PROPERTIES

3.2.1. Fresh Concrete Properties. Various tests were conducted on the fresh concrete prior to casting the test specimens. The type of fresh concrete test was dependent on the type of concrete being tested. A slump test was performed on all the concrete mixes upon arrival of the concrete mixing truck in accordance with ASTM C143/C143M “Standard Test Method for Slump of Hydraulic-Cement Concrete” (ASTM C143/C143M, 2010). A standard mold for the slump test was dampened and placed on a metal slump pan. Then the mold was filled to one-third of its volume with the fresh concrete. The concrete was then rodded 25 times uniformly over the cross section with a standard tamping rod. This process was repeated for the subsequent two layers. Upon finishing the last layer, the top of the concrete was smoothed using the tamping rod and any excess concrete was removed from around the base of the mold. The mold was then lifted vertically slowly in accordance with the ASTM. The length that the top of the fresh concrete slumped upon removal of the mold was recorded as the slump of the concrete. The slump test is shown in **Figure 3.1**.



Figure 3.1 – Slump test

The unit weight and air content were also determined. The unit weight of the fresh concrete was determined in accordance with ASTM C138/C138M “Standard Test Method for Density (Unit Weight), Yield, and Air Content (Gravimetric) of Concrete” (ASTM C138/C138M, 2010). A steel cylindrical container was used as the measure for this test. The inside of the measure was first dampened, and then it was weighed and measured to determine its empty weight and volume, respectively. Then fresh concrete was added to the measure to one-third of its volume. The concrete was then rodded 25 times with a standard tamping rod and the measure was struck with a rubber mallet 15 times around its outside perimeter. This step was repeated for the second and third level of concrete. Upon filling the measure, the concrete was finished with a strike-off plate and any excess concrete was removed from the rim of the measure using a sponge. The measure was then weighed to determine its weight and the weight of the concrete it contained. The weight of the measure was then subtracted from the combined weight of

the measure and the concrete to determine the weight of the concrete. The weight of the concrete was then divided by the volume of the measure to determine the unit weight of the concrete.

The air content of the concrete was determined in accordance with ASTM C231/C231M “Standard Test Method for Air Content of Freshly Mixed Concrete by the Pressure Method” (ASTM C231/C231M, 2010). A standard type-B meter was used for this test. The same steel container and filling procedure used for determining the unit weight were used for the air content test. After completing the filling process, the flange of the cover assembly was thoroughly cleaned and clamped onto the steel container. Both petcocks were opened and water was added to one petcock until the water emerged from the other petcock to remove any excess air in the steel container. The air bleeder valve was then closed and air was pumped into the container until the gauge hand was on the initial pressure line. Both petcocks were then closed and the main air valve was opened while simultaneously tapping the container smartly with a rubber mallet. The air content shown on the gauge was then recorded as the air content of the concrete.

3.2.2. Compressive Strength of Concrete. The concrete compressive strength was determined in accordance with ASTM C39/39M “Standard Test Method for Compressive Strength of Cylindrical Concrete Specimens” (ASTM C39/C39M, 2011). The specimens consisted of 4 in. (102 mm) diameter, 8 in. (203 mm) tall cylinders for each mix design. **Figure 3.2** displays the cylinders being cast. Prior to testing, the cylinders were capped in order to eliminate the effect of point stresses caused by an uneven surface. The capped cylinders were then subjected to a compressive axial load across their entire circular cross section until failure, applied at a rate appropriate for the

testing apparatus and in conformance with ASTM C39/C39M. The test setup is shown in **Figure 3.3**.



Figure 3.2 – Casting compressive strength cylinders



Figure 3.3 – Compressive strength test setup

3.2.3. Modulus of Rupture of Concrete. The modulus of rupture was determined in accordance with ASTM C78/C78M “Standard Test Method for Flexural Strength of Concrete (Using Simple Beam Third-Point Loading) (ASTM C78/C78M, 2010). The test consists of subjecting a 6 in. x 6 in. x 24 in. (152 mm x 152 mm x 610 mm) concrete beam to a four-point load until failure. **Eq. 3.1** was used to determine the modulus of rupture from each beam test result.

$$R = \frac{PL}{bd^2} \quad (3.1)$$

Where R is the modulus of rupture, P is the maximum applied load, L is the span length, b is the average width of the specimens at the fractured surface, and d is the average depth of the specimen at the fractured surface. The test specimens are shown in **Figure 3.4** and the test setup is shown in **Figure 3.5**.



Figure 3.4 – Modulus of rupture test specimens



Figure 3.5 – Modulus of rupture test setup

3.2.4. Splitting Tensile Strength of Concrete. The splitting tensile strength was determined in accordance with ASTM C496/C496M “Standard Test Method for Splitting Tensile Strength of Cylindrical Concrete Specimens” (ASTM C496/C496M, 2011). The specimens consisted of 6 in. (152 mm) diameter, 12 in. (305 mm) tall cylinders for each mix design, which were tested upon reaching the appropriate concrete compressive strength. **Eq. 3.2** was used to determine the splitting tensile strength of each cylinder test result.

$$T = \frac{2P}{\pi ld} \quad (3.2)$$

Where T is the splitting tensile strength, P is the maximum applied load, l is the length of the specimen, and d is the diameter of the specimen. The splitting tensile strength test setup is shown in **Figure 3.6**.



Figure 3.6 – Splitting tensile strength test setup

3.3. HIGH-VOLUME FLY ASH (HVFA) CONCRETE MIX DESIGNS

There were three concrete mix designs evaluated in the HVFA concrete test program. Two HVFA concrete mix designs were compared to a standard Missouri Department of Transportation (MoDOT) mix design in this study. All three mix designs had a target air content of 6% and a target slump of 4 to 5 in. (100 to 130 mm). The air entraining admixture consisted of MB-AE-90, and the water reducing admixture consisted of Glenium 7500, both manufactured by BASF and both approved for use in MoDOT projects. Gypsum and lime were added to the HVFA concrete mixes to increase early-age strength gain. The gypsum prevents sulfate depletion, and the lime provides the byproduct normally produced during cement hydration and necessary for the pozzolanic reaction of the fly ash.

3.3.1. HVFA Control Mix Design and Concrete Properties. The HVFA control mix design was designated HVFA-C and is shown in **Table 3.1**.

The slump, air content, and unit weight of the concrete used for the fabrication of test specimens was determined upon arrival of the concrete mixing truck. The slump measured 5 in. (127 mm), the air content measured 6.5%, and the unit weight measured 143.6 lb./ft³ (2300 kg/m³).

Test specimens for determining the compressive strength and modulus of rupture of the concrete were fabricated along with the bond test specimens. The compressive strength results are shown in **Table 3.2** and plotted in **Figure 3.7**. The splitting tensile strength results are shown in **Table 3.3**. The modulus of rupture test results are shown in **Table 3.4**.

Table 3.1 – HVFA-C mix proportions

Ingredient	Weight (lb./yd³)
w/cm	0.40
Cement (Type 1)	564
Coarse Aggregate	1,860
Fine Aggregate	1,240
MB-AE-90	0.625 oz./cwt.
Glenium 7500	2.5 oz./cwt.

Conversion: 1 lb./yd³ = 0.59 kg/m³
1 oz. = 29.6 ml
1 lb. = 0.45 kg

Table 3.2 – Compressive strength data of HVFA-C

Day	Average Strength (psi)
1	2,850
3	4,050
6	4,480

Conversion: 1 psi = 6.9 kPa

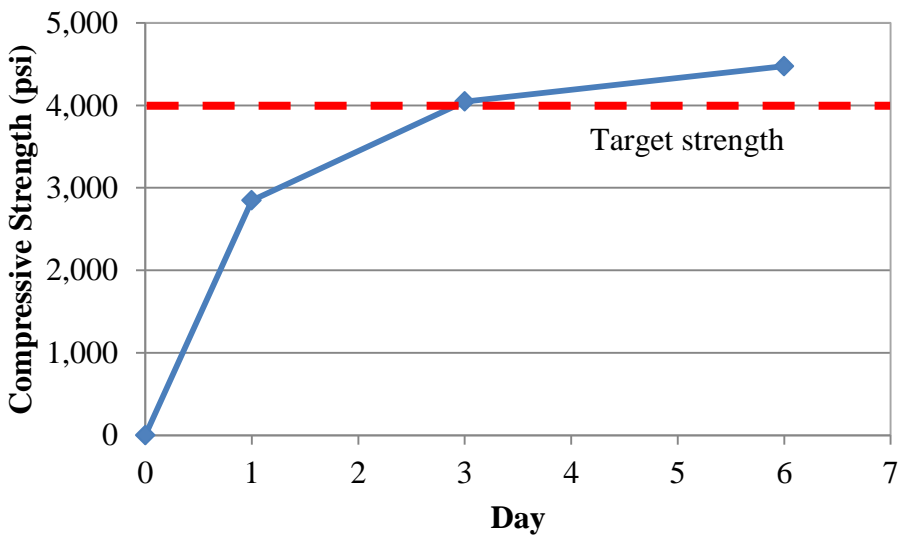


Figure 3.7 – Plot of HVFA-C compressive strength

Conversion: 1 psi = 6.9 kPa

Table 3.3 – Splitting tensile strength test results for HVFA-C

Specimen	Peak Load (lb.)	Splitting Tensile Strength (psi)
HVFA-C1	41,620	365
HVFA-C2	36,520	320
HVFA-C3	35,410	310
Average:		330

Conversion: 1 lb. = 4.45 N

1 psi = 6.9 kPa

Table 3.4 – Modulus of rupture test results for HVFA-C

Specimen	Peak Load (lb.)	Modulus of Rupture (psi)
HVFA-C1	4,560	380
HVFA-C2	4,720	390
HVFA-C3	5,495	460
HVFA-C4	5,450	430
Average:		415

Conversion: 1 lb. = 4.45 N

1 psi = 6.9 kPa

3.3.2. HVFA 70% Replacement, High Cementitious Material Mix Design and Concrete Properties. The HVFA 70% replacement, high cementitious material mix design was designated HVFA-70H and is shown in **Table 3.5**.

The slump and unit weight of the concrete used for the fabrication of test specimens was determined upon arrival of the concrete mixing truck. The slump measured 4.5 in. (114 mm) and the unit weight measured 142.5 lb./ft³ (2280 kg/m³).

Table 3.5 – HVFA-70H mix proportions

Ingredient	Weight (lb./yd³)
w/cm	0.40
Cement (Type 1)	230
Coarse Aggregate	1,754
Fine Aggregate	1,016
Fly Ash (Class C)	537
Gypsum	24
Calcium Hydroxide	60
Glenium 7500	2.5 oz./cwt.

Conversion: 1 lb./ yd³ = 0.59 kg/m³

1 oz. = 29.6 ml

1 lb. = 0.45 kg

Test specimens for determining the compressive strength, splitting tensile strength, and modulus of rupture of the concrete were fabricated along with the bond test specimens. The concrete compressive strength results are shown in **Table 3.6** and plotted in **Figure 3.8**. The splitting tensile strength test results are shown in **Table 3.7**. The modulus of rupture results are shown in **Table 3.8**.

Table 3.6 – Compressive strength data of HVFA-70H

Day	Average Strength (psi)
1	710
3	1,505
7	2,400
14	2,955
28	3,100
56	3,420

Conversion 1 psi = 6.9 kPa

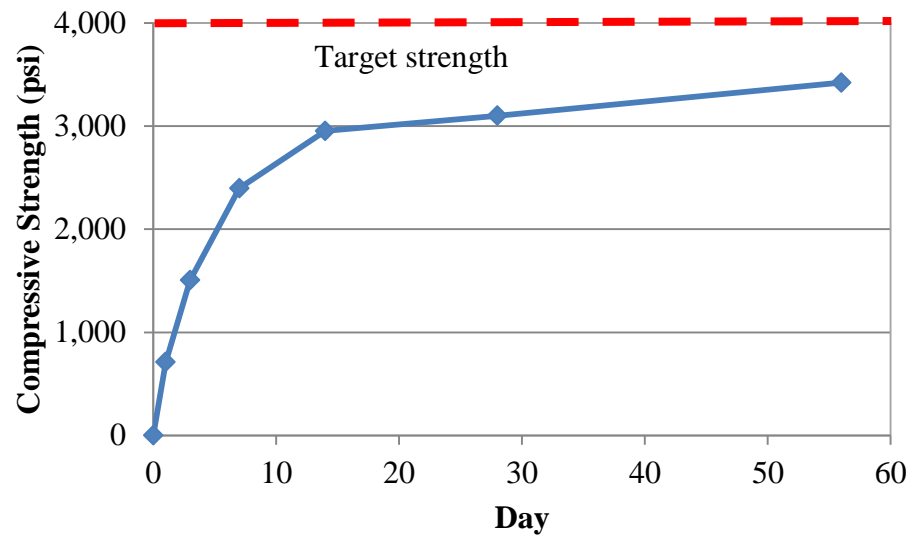


Figure 3.8 – Plot of HVFA-70H compressive strength
Note: 1 psi = 6.9 kPa

Table 3.7 – Splitting tensile strength test results for HVFA-70H

Specimen	Peak Load (lb.)	Splitting Tensile Strength (psi)
HVFA-70H1	31,635	280
HVFA-70H2	26,550	235
HVFA-70H3	32,865	290
Average:		300

Note: 1 lb. = 4.45 N
1 psi = 6.9 kPa

Table 3.8 – Modulus of rupture test results for HVFA-70H

Specimen	Peak Load (lb.)	Modulus of Rupture (psi)
HVFA-70H1	4,315	350
HVFA-70H2	4,120	345
HVFA-70H3	4,085	340
HVFA-70H4	4,515	365
Average:		350

Conversion: 1 lb. = 4.45 N

1 psi = 6.9 kPa

3.3.3. HVFA 70% Replacement, Low Cementitious Material Mix Design and

Concrete Properties. The HVFA 70% replacement, low cementitious material mix design was designated HVFA-70L and is shown in **Table 3.9**.

The slump and unit weight of the concrete used for the fabrication of test specimens was determined upon arrival of the concrete mixing truck. The slump measured 4.5 in. (114 mm) and the unit weight measured 149.6 lb./ft³ (2400 kg/m³).

Table 3.9 – HVFA-70L mix proportions

Ingredient	Weight (lb./yd ³)
w/cm	0.40
Cement (Type 1)	155
Coarse Aggregate	1,860
Fine Aggregate	1,240
Fly Ash (Class C)	360
Gypsum	18
Calcium Hydroxide	49
Glenium 7500	4 oz./cwt.

Conversion: 1 lb./ yd³ = 0.59 kg/m³

1 oz. = 29.6 ml

1 lb. = 0.45 kg

Test specimens for determining the compressive strength, splitting tensile strength, and modulus of rupture of the concrete were fabricated along with the bond test specimens. The concrete compressive strength test results are shown in **Table 3.10** and plotted in **Figure 3.9**. The splitting tensile strength results are shown in **Table 3.11**. The modulus of rupture test results are shown in **Table 3.12**.

Table 3.10 – Compressive strength data of HVFA-70L

Day	Average Strength (psi)
1	820
3	1,815
7	2,750
14	3,235
28	3,480
33	3,450

Conversion: 1 psi = 6.9 kPa

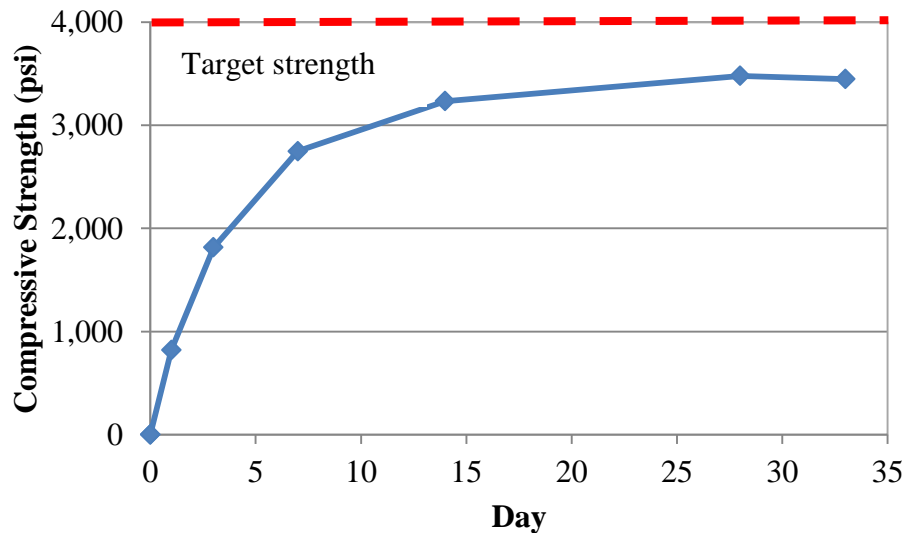


Figure 3.9 – Plot of HVFA-70L compressive strength
Conversion: 1 psi = 6.9 kPa

Table 3.11 – Splitting tensile strength test results for HVFA-70L

Specimen	Peak Load (lb.)	Splitting Tensile Strength (psi)
HVFA-70L1	34,530	305
HVFA-70L2	35,235	310
HVFA-70L3	33,075	290
Average:		300

Conversion: 1 lb. = 4.45 N

1 psi = 6.9 kPa

Table 3.12 – Modulus of rupture test results for HVFA-70L

Specimen	Peak Load (lb.)	Modulus of Rupture (psi)
HVFA-70L1	5,290	420
HVFA-70L2	5,570	460
HVFA-70L3	5,140	425
HVFA-70L4	5,080	425
Average:		430

Conversion: 1 lb. = 4.45 N

1 psi = 6.9 kPa

4. EXPERIMENTAL PROGRAM

4.1. INTRODUCTION

The experimental program included both direct pull-out tests, as well as well as full-scale beam splice specimen tests. The direct pull-out specimens were based on RILEM 7-II-128 “RC6: Bond test for reinforcing steel. 1. Pull-out test” (RILEM, 1994). The beam splice specimen tests were based on recommendations in ACI 408R-03 “Bond and Development of Straight Reinforcing Bars in Tension” (ACI 408R-03, 2003). The following is a discussion of the design, setup, instrumentation, and procedures for both testing methods.

4.2. DIRECT PULL-OUT TEST

4.2.1. Direct Pull-out Specimen Design. The direct pull-out specimen tests were based on the RILEM 7-II-128 “RC6: Bond test for reinforcing steel. 1. Pull-out test” (RILEM, 1994). Several changes were made to the recommended test specimen based on results from previous research (Wolfe, 2011). The test involves casting a length of reinforcing bar within a concrete cylinder and applying a direct tension force on the bar until the bonded length fails. Although not directly related to the behavior of a reinforced concrete beam in flexure, the test does provide a realistic comparison of bond between types of concrete.

The RILEM standard states that the reinforcing bar will be embedded in the concrete a total length of 15 times the bar diameter to be tested. A bond breaker a length of 7.5 times the bar diameter is to be placed so that the bar is unbonded from the bottom

surface to halfway in the concrete, leaving a bonded length of 7.5 times the bar diameter. The unbounded length at the bottom of the concrete segment is to reduce restraint stresses caused by friction with the loading head. Previous testing showed this bonded length to be too long and yielding of the bar occurred prior to failure in some instances (Wolfe, 2011). To ensure the bond failed before the bar yielded, the total concrete depth was reduced to 10 times the bar diameter with a bonded length of 5 times the bar diameter.

The RILEM standard specifies a square concrete cross section with sides having a length of 8.75 in. (222 mm). For this test program, a circular concrete cross section with a diameter of 12 in. (305 mm) was used instead. This change eliminated the potential for a splitting failure (side cover failure) and also maintained a constant cover for the reinforcing bar.

The protocol for the direct pull-out tests included two bar sizes – #4 (#13) and #6 (#19) – in order to evaluate the bond performance over a range of reinforcing sizes. The total length of each bar was 40 in (1016 mm). A length of 3/8 in. (10 mm) was left exposed at the top of the specimen to measure bar slip using a Linear Voltage Differential Transformer (LVDT). **Figures 4.1** and **4.2** are schematic diagrams of the specimen dimensions for the #4 (#13) and #6 (#19) bars, respectively.

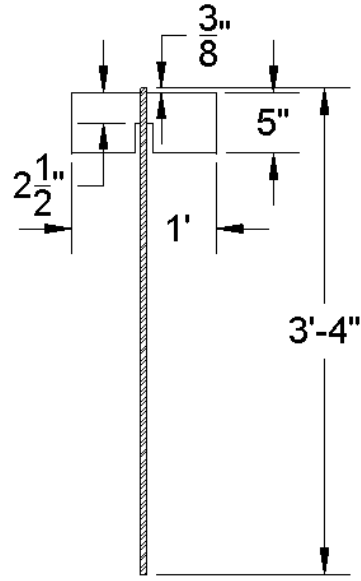


Figure 4.1 – Pull-out specimen with dimensions for #4 (#13) reinforcing bars
Conversion: 1 in. = 25.4 mm

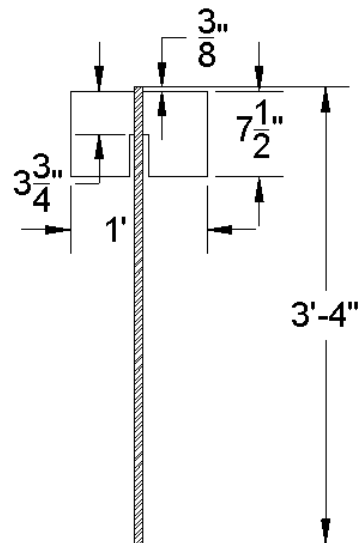


Figure 4.2 – Pull-out specimen with dimensions for #6 (#19) reinforcing bars
Conversion: 1 in. = 25.4 mm

4.2.2. Direct Pull-out Specimen Fabrication. The formwork base for the direct pull-out test specimen was constructed with a 14-in.-square (356 mm), 3/8-in.-thick (10 mm) section of plywood. A hole that was 1/16 in. (0.16 mm) larger than the bar diameter being tested was drilled through the center of the plywood squares. Cardboard tubing (Quick-Tube) was then cut to the required length, depending on the bar size being tested. Waterproof silicone adhesive caulk was then used to bind the cardboard tubing to the plywood squares.

The reinforcing bar for each specimen was sectioned into 40 in. (1016 mm) lengths. Polyvinyl chloride (PVC) tubing was used to form the bond breaker. For the #4 (#13) bar, the PVC had an inside diameter of 3/4 in. (19 mm) and was sectioned into lengths of 2.5 in. (64 mm). For the #6 (#19) bar, the PVC had an inside diameter of 1 in. (25 mm) and was sectioned into 2.75 in. (70 mm) lengths. A mark was made on each bar to facilitate the placement of the PVC bond breaker. The PVC was slid onto the reinforcing bar and shims of cardboard were used to center the bar in the PVC. The PVC was then adhered to the reinforcing bar using waterproof silicone adhesive caulk and was carefully finished to ensure there were no gaps in the caulk for the concrete paste to get between the bar and the PVC.

The top of the formwork was also a 14-in.-square (356 mm) of 3/8-in.-thick (10 mm) plywood with a hole drilled through its center. To ensure that the bars were plumb within the concrete encasement, prior to constructing the specimens, the reinforcing bars were placed in the completed forms and leveled. Upon leveling the bars, an outline of the cylindrical form was drawn on the underside of the top plywood square. Wood spacers were then screwed into the plywood square along the outline of the cardboard tubing.

The specimens were cast by first placing the reinforcing bar through the hole in the base of the formwork. Concrete was then placed in the cylindrical formwork and consolidated as necessary. After proper placement of the concrete, the exposed surface was finished. The top of the formwork was then carefully slid down the reinforcing bar and the wood spacers were fit snugly over the cylindrical forms. The reinforcing bar was checked to ensure it was plumb and then the sides of the cylindrical forms were lightly vibrated. The pull-out and companion material property specimens were allowed to cure until the concrete reached its specified strength prior to testing. The cardboard tubing was removed on the day of testing. Construction of the pull-out specimens is shown in **Figure 4.3**, with complete specimens shown in **Figure 4.4**.



Figure 4.3 – Pull-out specimen construction



Figure 4.4 – Completed specimens

4.2.3. Direct Pull-out Test Setup. Testing of the direct pull-out specimens was completed using a 200,000-lb-capacity (890 kN) testing machine manufactured by Tinius Olson. The test setup is shown in **Figures 4.5** and **4.6**. The cylindrical forms were removed immediately prior to testing. A neoprene pad with a hole in its center was placed on the top platform of the test machine to ensure uniform bearing of the concrete. The specimens were flipped upside down and the reinforcing bar was then threaded through the hole in the neoprene pad on the top platform and placed between the grips installed on the middle platform. An LVDT was then clamped to a stand, and the stand was placed on top of the concrete section of the specimen. The needle of the LVDT was placed on top of the 3/8 in. (10 mm) length of exposed reinforcing bar to measure slip.

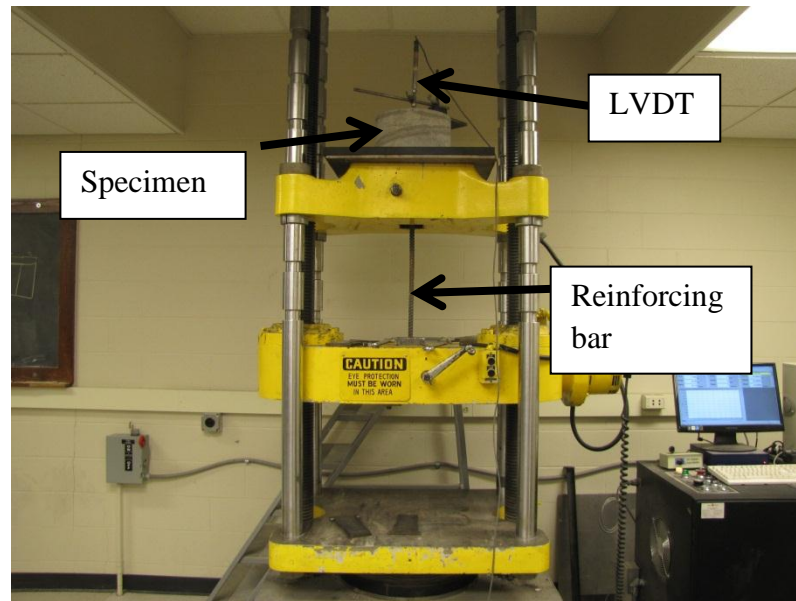


Figure 4.5 – Direct pull-out test setup

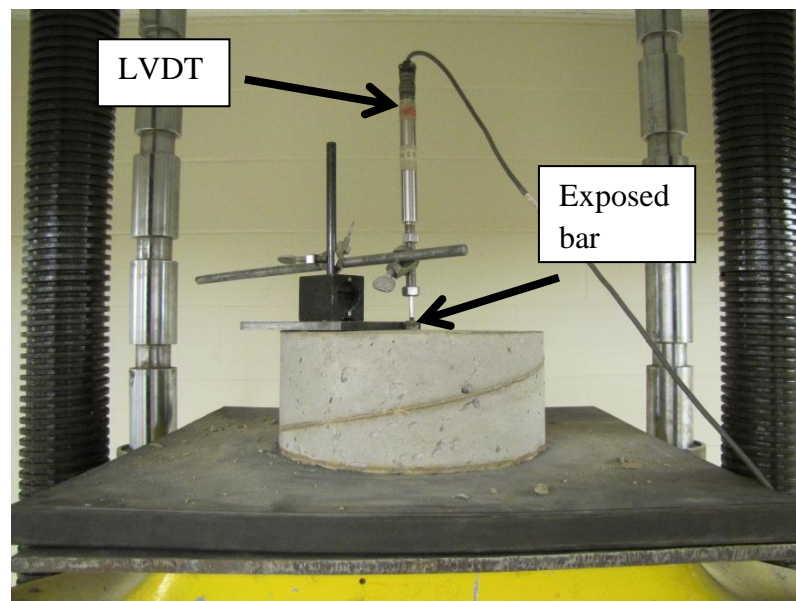


Figure 4.6 – LVDT installation to measure bar slip

4.2.4. Direct Pull-out Test Procedure. The middle platform was manually positioned to allow for the reinforcing bar to be clamped. The equipment controlling the

Tinius Olson was programmed to apply a displacement controlled load rate of 0.1 in. (3 mm) per minute. Upon initiating a new test, the LVDT data collection platform was started and the clamps were closed around the reinforcing bar while the middle platform was simultaneously lowered. This step was done to seat the test specimen and apply an initial load sufficient to maintain a proper grip on the reinforcing bar during testing. The test program was then initiated and allowed to run until a distinct peak was observed in the applied load vs. bar slip plot. This step was done to ensure there was no residual load carrying capacity in the bonded region and that the proper failure load was determined. At that point, the test program and LVDT data collection platform were both stopped and the test specimen was removed.

4.3. BEAM SPLICE TEST

4.3.1. Beam Splice Specimen Design. The beam splice test specimens were designed following a non-ASTM test procedure that is generally accepted as the most realistic test method for both development and splice length. This test consists of applying a full-scale beam specimen to a four-point loading until failure of the splice occurs. The splice is located in the region of the beam subjected to a constant moment, and thus constant stress. The realistic stress-state in the area of the reinforcing bars makes for an accurate representation of the bond strength of the tested member (ACI 408R-03, 2003).

Details of the beam splice specimens used in this current study are shown in **Figures 4.7** and **4.8**. The beams measured 10 ft. (3050 mm) in length, with a cross section of 12 in. x 18 in. (305 mm x 457 mm) and contained a splice centered at midspan.

Transvers steel consisting of #3 (#10), ASTM A615-09, Grade 60, U-shaped stirrups were used for shear reinforcement. A stirrup spacing less than the ACI 318-08 maximum stirrup spacing was used to ensure that bond failure occurred prior to shear failure. The stirrups were terminated at approximately 5 in. (127 mm) from each end of the splice to eliminate the effects of confinement within the splice region. The longitudinal reinforcement consisted of three, ASTM A615-09, Grade 60, #6 (#19) bars spliced at midspan of the beam. The splice length was based on a percentage of the development length of the longitudinal reinforcing bars calculated in accordance with ACI 318-08 “Building Code Requirements for Structural Concrete” (ACI 318-08, 2008) (**Eq. 4.1**).

$$l_d = \left(\frac{3}{40} \frac{f_y}{\lambda \sqrt{f'_c}} \frac{\Psi_t \Psi_e \Psi_s}{\left(\frac{c_b + K_{tr}}{d_b} \right)} \right) d_b \quad (4.1)$$

Where l_d is the development length, f_y is the specified yield strength of reinforcement, λ is the lightweight concrete modification factor, f'_c is the specified compressive strength of concrete, Ψ_t is the reinforcement location modification factor, Ψ_e is the reinforcement coating modification factor, Ψ_s is the reinforcement size modification factor, c_b is the smaller of the distance from center of a bar to nearest concrete surface and one-half the center-to-center spacing of bars being developed, K_{tr} is the transverse reinforcement index, and d_b is the nominal diameter of the reinforcing bar.

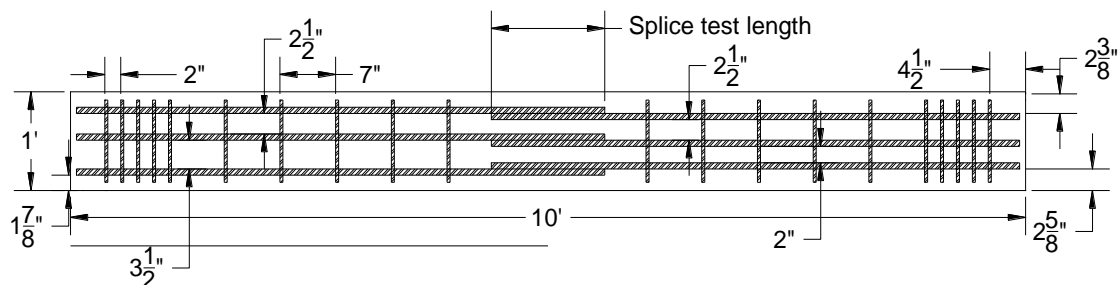


Figure 4.7 – Beam splice specimen reinforcing layout

Conversion: 1 in. = 25.4 mm

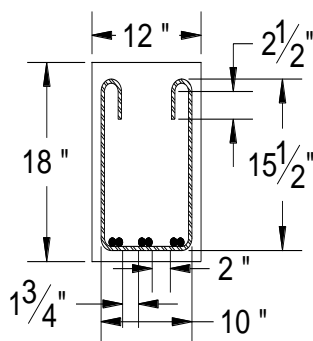


Figure 4.8 – Beam splice specimen cross section

Conversion: 1 in. = 25.4 mm

To ensure bond failure before yielding of the reinforcing bar, a splice length less than the code required development length was used in the test specimen. Prior researchers used one-half of a Class B splice as the lap length (Wolfe, 2011). However, several test specimens in that study exhibited signs of yielding in the reinforcement prior to bond failure. Therefore, for this current study, the splice length was limited to 70% of the development length.

4.3.2. Beam Splice Specimen Fabrication. The concrete formwork consisted of five removable and reusable pieces constructed from steel and wood. The pieces were connected through the use of steel keys and wire ties were used to hold the keys in place. The original beam forms were 14 ft. (4267 mm) in length. Consequently, 4 ft. (1219 mm)

wooden bulkheads were constructed to reduce the length of the beam forms to 10 ft. (3048 mm).

The #3 (#10) reinforcing bars were then sectioned to the appropriate length and bent to form the U-stirrups. The longitudinal reinforcement was sectioned to the appropriate length to obtain the proper splice length, as well as create a standard hook at the opposite end for proper development. All rust and mill scale was removed from the spliced region of each bar using a wire brush cup attached to an electric grinder. This step was done to ensure the bond strength was not affected in any way by the existence of rust and mill scale, thus maintaining conformity between the splice in each specimen. The longitudinal bars were then placed on saw-horses, aligned to obtain the appropriate splice length, and the stirrups were secured to the longitudinal bars using steel wire ties. A strain gauge was attached to the longitudinal bars at one end of each splice to monitor the strain during testing. Then, to ensure the stirrups stayed aligned vertically within the forms, two #4 (#13) bars were tied to the top bend of the stirrups and the end stirrups were tied to the hooked ends of the longitudinal bars. A finished reinforcing bar cage is shown in **Figure 4.9**.



Figure 4.9 – Finished reinforcing bar cage

Two of the cages were then lowered into the beam forms using 1 in. (25 mm) steel chairs on the bottom and sides to maintain 1 in. (25 mm) of clear cover to the outside edge of the stirrups. The third cage was turned upside down and 1.5 in. (38 mm) chairs were attached to the bottom of the cage to maintain clear cover to the splice at the top of the beam. Then, 1 in. (25 mm) chairs were also attached to the side of the stirrups to maintain 1 in. (25 mm) clear cover to the stirrups. Steel crossties were attached to the tops of the beam forms to maintain the proper beam width along the depth of the beam. Hooks were then tied to the crossties to facilitate transportation of the specimen after curing. **Figure 4.10** shows a picture of the spliced region in the beam forms, and **Figure 4.11** displays the three cages in their respective forms.

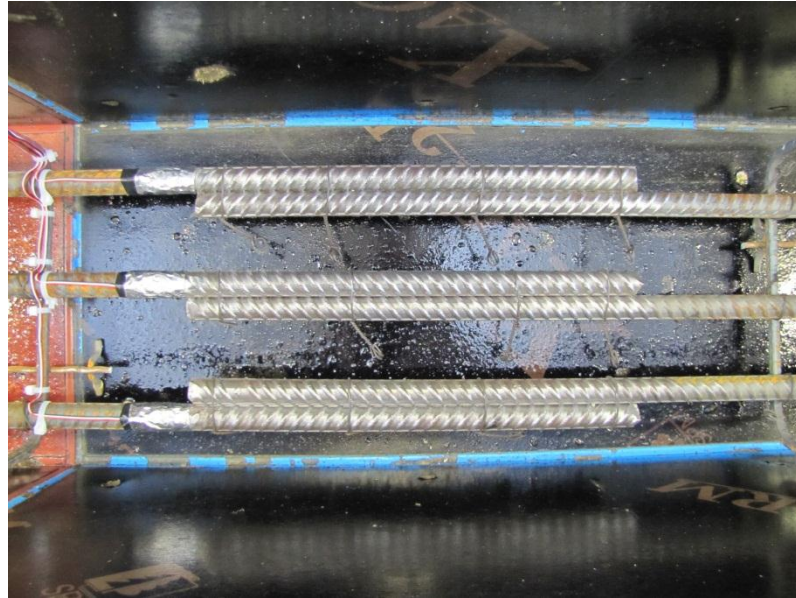


Figure 4.10 – Spliced longitudinal bars for normal strength concrete



Figure 4.11 – Reinforcing bar cages in beam forms

The concrete used to construct the specimens was delivered from a local ready-mix facility, Rolla Ready Mix (RRM). The mix design was supplied to RRM although

some of the water was held in abeyance in order to adjust the water content at the lab. Once the concrete truck arrived at the lab, the slump was measured and the reserve water was added as necessary to arrive at the required water-to-cementitious material ratio. At that point, all necessary activators and admixtures were added to the concrete truck, which was then mixed at high speed for 10 minutes to obtain the final material. At this point, the fresh concrete was loaded into a concrete bucket as shown in **Figure 4.12**. The bucket was then positioned with the overhead crane to facilitate placement of the concrete into the formwork as shown in **Figure 4.13**. The concrete was then consolidated as required for the particular concrete mix. This process was repeated until the beam forms were filled. The tops of the beams were then finished using trowels as shown in **Figure 4.14**.



Figure 4.12 – Concrete bucket being filled with fresh concrete



Figure 4.13 – Placement of concrete into beam forms

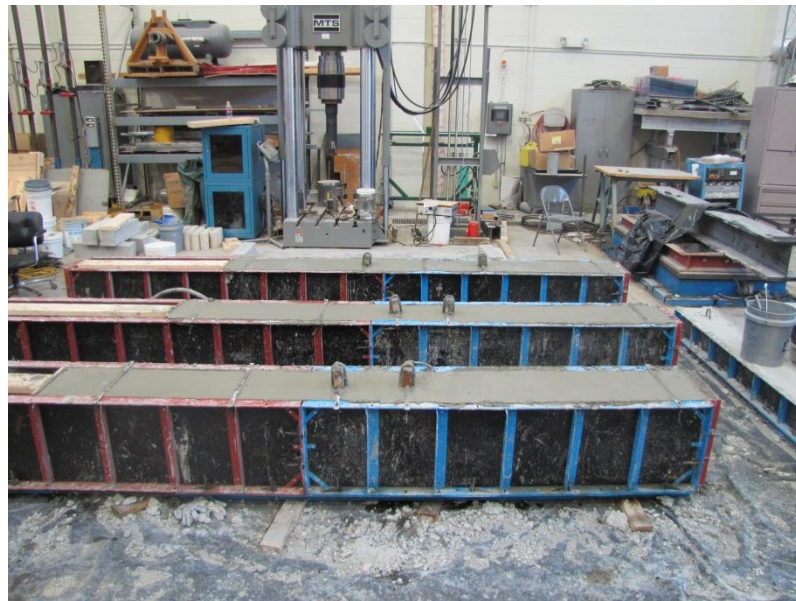


Figure 4.14 – Finished beams in forms

Once the concrete reached initial set, the beam specimens and companion material property specimens were covered with wet burlap and plastic. The specimens were

allowed to cure until the concrete compressive strength reached a minimum of 1500 psi (10.3 MPa), at which point they were removed from the forms and remained within the temperature-controlled High Bay Lab. The beams were then tested upon reaching their respective design compressive strengths.

4.3.3. Beam Splice Specimen Test Setup. A schematic and photograph of the test setup are shown in **Figures 4.15** and **4.16**, respectively. The test consists of subjecting the beam splice specimen to four-point loading, ensuring that the region containing the splice is located in a constant moment region. The beam was then placed onto the supports. Two steel rollers were placed on the top surface of the beam specimen and steel spreader beams were used to transfer the applied load from two 140-kip-capacity (623 kN) hydraulic actuators.

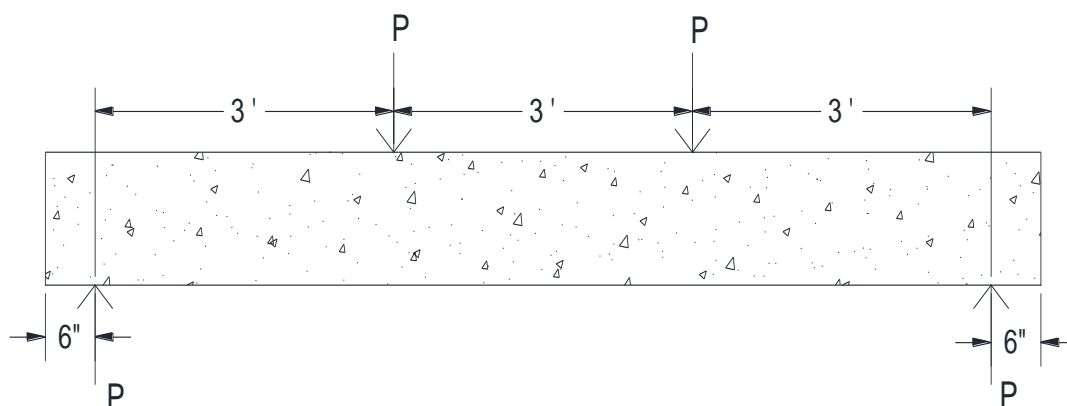


Figure 4.15 – Beam loading schematic

Conversion: 1 in. = 25.4 mm

The process of installing the beams into the test setup started with marking the center point, load points, and spreader beam outline onto each specimen. The strain gauge wires were then attached to a strain gauge converter box for subsequent attachment to the data acquisition system. At this point, the overhead crane was used to transport the beams

to a location adjacent to the test setup. The beams were then lowered onto steel rollers to facilitate placement into the test setup. The beam was then rolled into a position where the center point mark was directly below the center web stiffener on the spreader beam. One end was lined up with the spreader beam, lifted off of the steel roller with a hydraulic jack, and then lowered onto the support. This process was then repeated for the other support to line the beam up properly in the test frame. Once the beam was positioned within the test frame, metal plates were installed at the load point marks and the transfer beam was lowered into place. **Figure 4.16** shows the beam in the load frame located at the Missouri S&T High-Bay Structures Laboratory. A segment of aluminum angle was attached to the midpoint of the beam and an LVDT was placed on the aluminum to measure the deflection at midspan during testing as shown in **Figure 4.17**. The strain gauge wire converter box was then attached to the data acquisition system.



Figure 4.16 – Beam positioned within load frame



Figure 4.17 – LVDT installation

4.3.4. Beam Splice Test Procedure. Prior to beginning the test, the data acquisition system was initiated to record applied load, LVDT data, and strain gauge data. The load was then applied by the two 140-kip-capacity (623 kN) hydraulic actuators acting through the spreader beams. Each test was performed under displacement control, and the load was applied in a series of loading steps of 0.02 in. (0.5 mm), which corresponded to a load of approximately 3 kips (13 kN), until failure. Electronic measurements of strain and deformation were recorded throughout the entire loading history of the specimens. The crack patterns in the concrete were marked at every other load step to track propagation as the load was increased. Loading of the beams continued until a very prominent failure occurred, which was usually signaled both audibly and by a significant drop in the load-deflection behavior of the specimen.

5. HVFA TEST RESULTS AND EVALUATION

5.1. DIRECT PULL-OUT TEST RESULTS

The direct pull-out test specimens were constructed to evaluate the bond performance of HVFA concrete. The MoDOT standard mix design was used as a baseline for test result comparisons. A total of 18 direct pull-out test specimens were constructed for the HVFA concrete test program. There were six test specimens constructed for each of the HVFA concrete mix designs, as well as for the control mix design. Of the six specimens constructed for each mix design, three specimens contained a #4 (#13) reinforcing bar and three specimens contained a #6 (#19) reinforcing bar. The test matrix for the HVFA concrete direct pull-out test program is shown in **Table 5.1**.

Table 5.1 – HVFA concrete direct pull-out test matrix

Mix I.D.	Bar Size	No. of Specimens
HVFA-C	#4 (#13)	3
	#6 (#19)	3
HVFA-70H	#4 (#13)	3
	#6 (#19)	3
HVFA-70L	#4 (#13)	3
	#6 (#19)	3

Due to the limitations of the local ready mix concrete plant, it was necessary to add the appropriate amount of powder activators (gypsum and calcium hydroxide) specified in each HVFA concrete mix design upon arrival of the mixing truck. The addition of calcium hydroxide can be seen in **Figure 5.1**.



Figure 5.1 – Adding calcium hydroxide to the mixing truck

The applied load and corresponding slip of each reinforcing bar through the surrounding concrete were recorded for each test. Once compiled, the maximum applied load (peak load) for each test specimen was determined and used for bond strength comparisons. **Table 5.2** displays the peak load for each of the test specimens in the HVFA concrete test program, as well as the average coefficient of variation (COV) for each group of data. The first number in the specimen name represents the bar size, the following PO designates that specimen as a pull-out specimen, and the final number is the number of the specimen. Plots of the peak load for the HVFA-C, HVFA-70H, and HVFA-70L specimens are shown in **Figures 5.2, 5.3, and 5.4**, respectively. The plots indicate that results from tests having the same parameters are relatively similar. This facet is also demonstrated by the relatively small COV within a group of test results, with the highest being 7%. The consistent results between tests with the same parameters lend

confidence in the ability of this test to accurately compare the bond strength between mix designs.

Table 5.2 – HVFA concrete pull-out test results

Mix	Bar Size	Specimen	Max Applied Load (lb.)	Average Applied Load (lb.)	COV (%)
HVFA-C	#4 (#13)	4PO1	10,002	10,270	6.8
		4PO2	11,058		
		4PO3	9,749		
	#6 (#19)	6PO1	24,289	24,784	3.6
		6PO2	24,234		
		6PO3	25,829		
HVFA-70H	#4 (#13)	4PO1	8,604	8,912	3.0
		4PO2	9,091		
		4PO3	9,042		
	#6 (#19)	6PO1	24,770	24,264	4.1
		6PO2	24,902		
		6PO3	23,120		
HVFA-70L	#4 (#13)	4PO1	9,989	9,243	7.1
		4PO2	8,750		
		4PO3	8,992		
	#6 (#19)	6PO1	23,120	23,817	4.7
		6PO2	25,108		
		6PO3	23,222		

Conversion: 1 lb. = 4.45 N

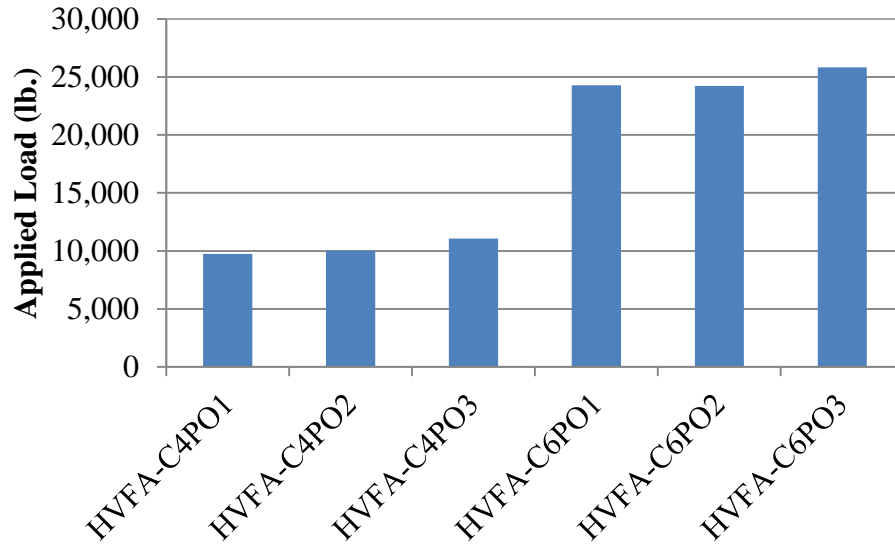


Figure 5.2 – HVFA-C pull-out test results
Conversion: 1 lb. = 4.45 N

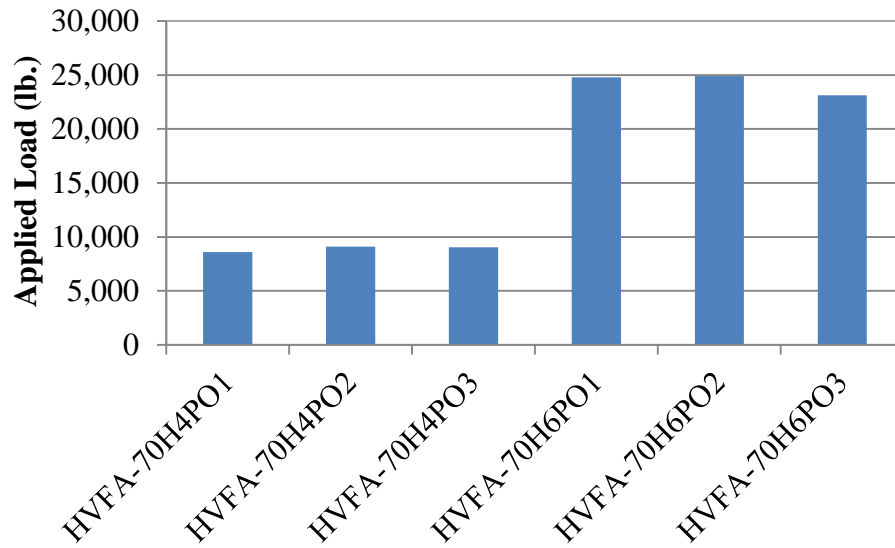


Figure 5.3 – HVFA-70H pull-out test results
Conversion: 1 lb. = 4.45 N

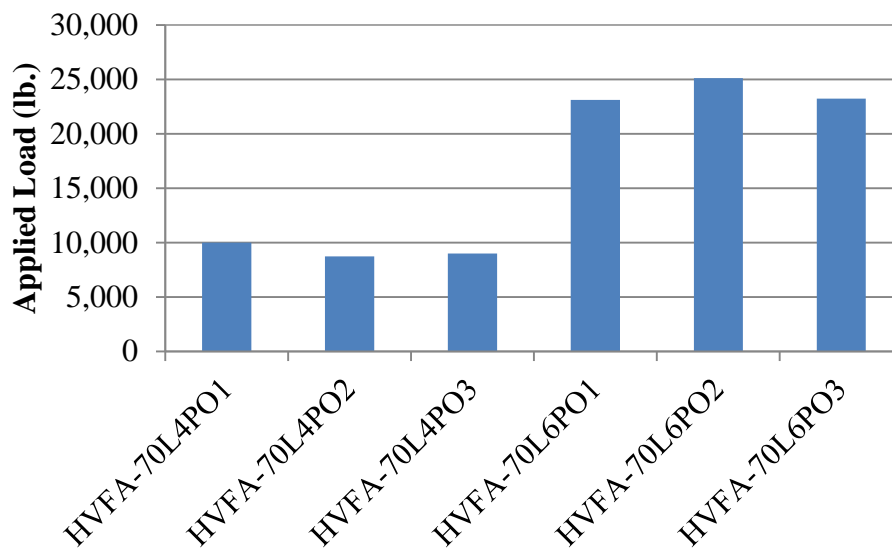


Figure 5.4 – HVFA-70L pull-out test results

Conversion: 1 lb. = 4.45 N

The load and bar slip data were also plotted for comparison. An example of a load vs. slip plot is shown in **Figure 5.5**. All other load vs. slip plots have a similar shape and only differ in the magnitude of the values plotted, with one exception. The most consistent mode of failure of the pull-out test specimens consisted of the reinforcing bar slipping through the concrete section. However, the test specimen HVFA-C6PO3 failed by splitting of the concrete section, as shown in **Figure 5.6**. This mode of failure was due to the reinforcing bar being noticeably out of plumb. The load vs. slip plot for HVFA-C6PO3 is shown in **Figure 5.7**. Appendix B contains the load vs. slip plots for all 18 pull-out specimens.

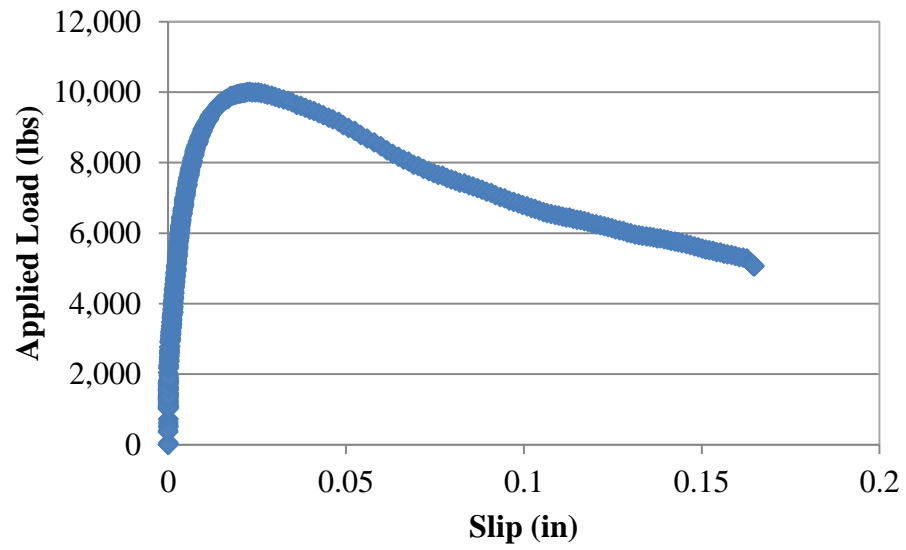


Figure 5.5 – Example applied load vs. slip plot
Conversion: 1 in. = 25.4 mm
1 lb. = 4.45 N



Figure 5.6 – HVFA-C6PO3 failed specimen

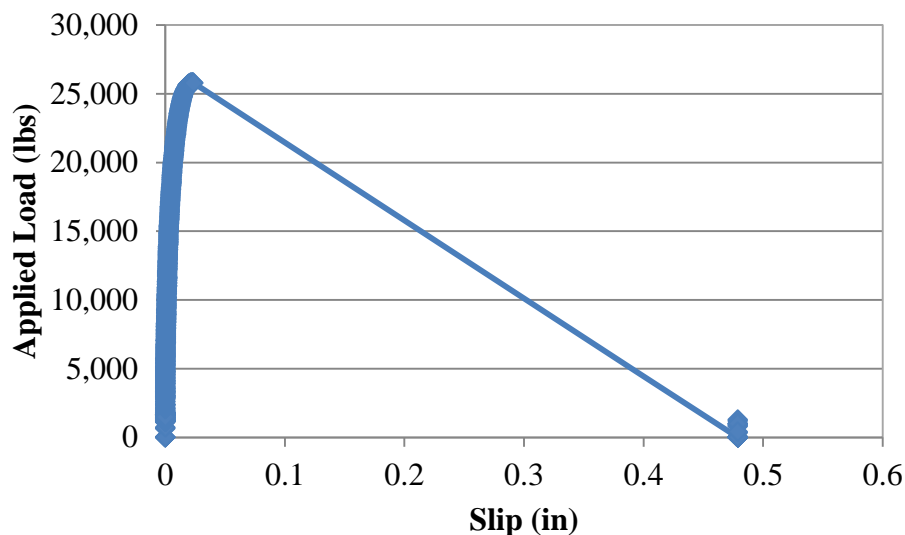


Figure 5.7 – HVFA-C6PO3 applied load vs. slip plot

Conversion: 1 in. = 25.4 mm

1 lb. = 4.45 N

5.2. BEAM SPLICE TEST RESULTS

The beam splice test specimens were constructed to evaluate the bond performance of HVFA concrete under more realistic loading conditions. The MoDOT standard mix design was used as a baseline for test result comparisons. A total of nine test specimens with 3#6 (#19) longitudinal reinforcing bars spliced at midspan were constructed for the HVFA concrete test program. There were three test specimens constructed for each of the two HVFA concrete mix designs to be evaluated, as well as for the control mix design. Of the three test specimens, two specimens were constructed with the spliced reinforcing bar located at the bottom of the beam cross section and one specimen was constructed with the splice at the top of the beam cross section to evaluate the top-bar effect. The test matrix for the HVFA concrete beam splice test program is shown in **Table 5.3**. A splice length of 14.34 in. (364 mm) was used for each test specimen.

Table 5.3 – HVFA concrete beam splice test matrix

Mix I.D.	Bar Size	Splice Location	No. of Specimens
HVFA-C	#6 (#19)	Bottom	2
		Top	1
HVFA-70H	#6 (#19)	Bottom	2
		Top	1
HVFA-70L	#6 (#19)	Bottom	2
		Top	1

The applied load, corresponding midspan deflection, and corresponding strain at the end of each bar splice were recorded for each test. The peak load and peak stress were collected for each test specimen and are shown in **Table 5.4**. The bottom splice specimens are denoted with the abbreviation BB and the top splice specimens are denoted with the abbreviation TB. Steel stress recorded at failure of the specimen was determined by averaging the strain readings from each strain gage in a member and finding the peak strain that occurred during loading. This peak strain was then multiplied by the average modulus of elasticity of the steel determined from the tension test to determine the peak stress. The peak loads for the HVFA-C, HVFA-70H, and HVFA-70L specimens are plotted in **Figures 5.8, 5.9, and 5.10**, respectively.

Table 5.4 – Peak load and reinforcing bar stresses

Mix	Specimen	Steel Stress Recorded at Failure (ksi)	Peak Load (kips)
HVFA-C	BB1	54.6	53.3
	BB2	48.6	49.7
	TB	48.1	49.5
HVFA-70H	BB1	62.4	55.9
	BB2	55.1	56.1
	TB	62.8	60.2
HVFA-70L	BB1	54.0	55.2
	BB2	49.9	51.1
	TB	51.7	55.1

Conversion: 1 ksi = 6.9 MPa

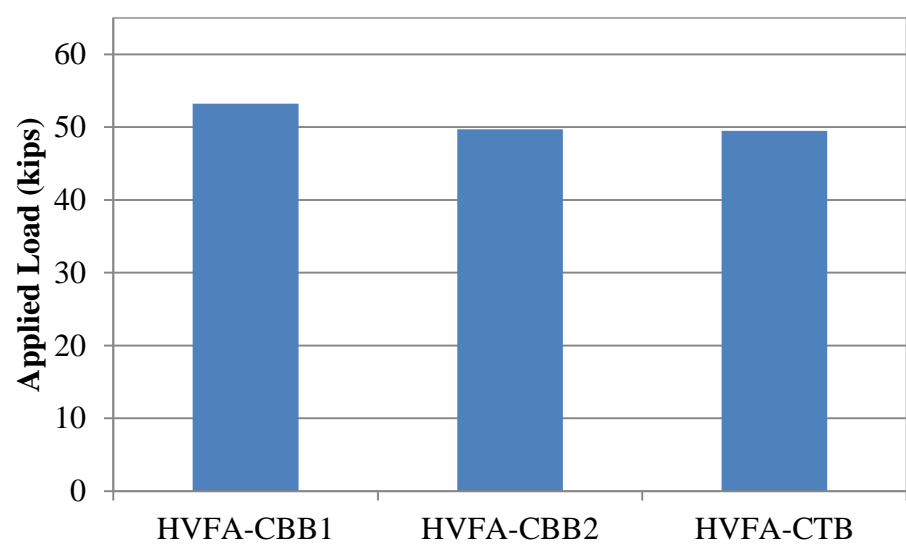


Figure 5.8 – HVFA-C peak load plot

Conversion: 1 kip = 4.45 kN

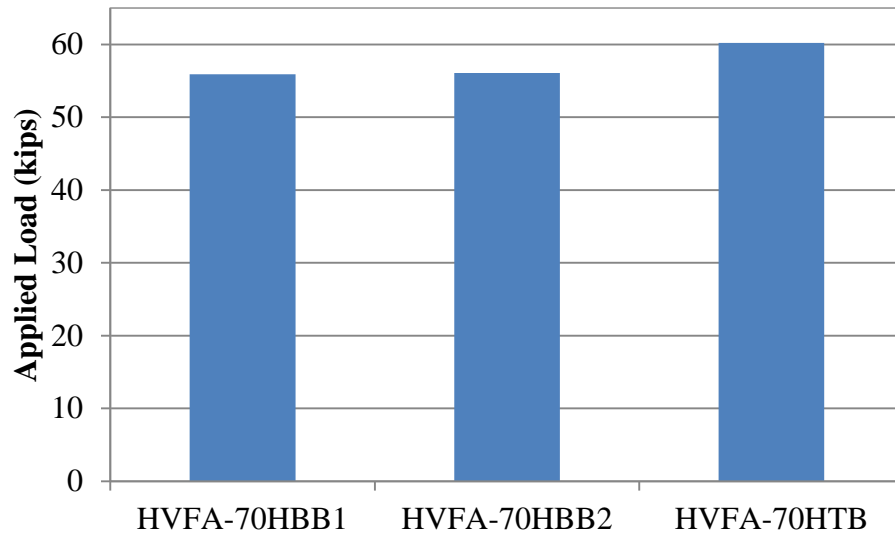


Figure 5.9 – HVFA-70H peak load plot
Conversion: 1 kip = 4.45 kN

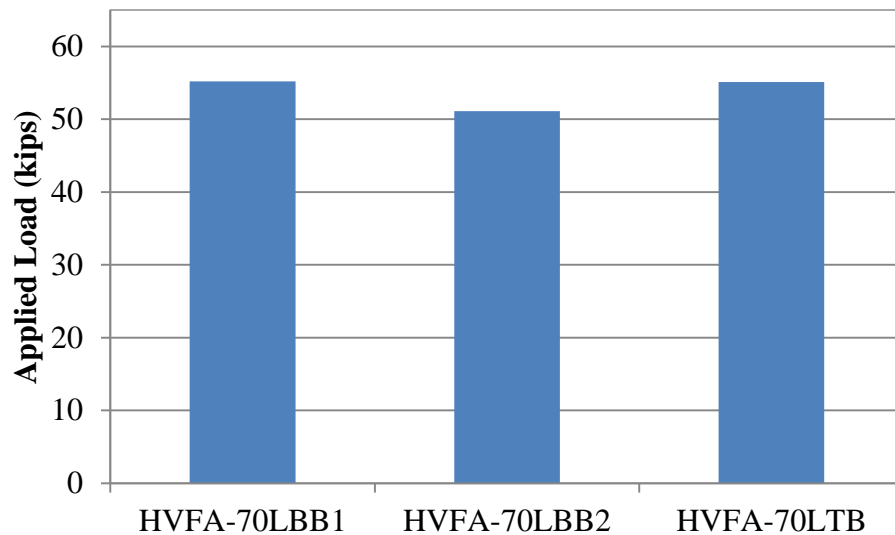


Figure 5.10 – HVFA-70L peak load plot
Conversion: 1 kip = 4.45 kN

The deflection and strain data were also plotted with the load data to observe the response of the specimens during testing. A typical load vs. displacement at midspan plot is shown in **Figure 5.11**. A typical load vs. strain plot is shown in **Figure 5.12**. The plots

shown are from the HVFA-CBB1 specimen. Both plots indicate that the beam began to develop flexural cracks at a load of approximately 12 kips (53 kN). At the failure load, all specimens exhibited visible and audible signs of complete bond failure, having never yielded the reinforcing bars. Evidence of this is shown in the linear behavior indicated in both the load vs. deflection plot and the load vs. strain plot. Appendix B contains the load vs. slip plots for all nine beam splice specimens.

The cracking patterns in the beam splice specimens also revealed a bond failure. For example, **Figures 5.13, 5.14, and 5.15** display the failed beam specimen designated HVFA-70HBB2. **Figures 5.14 and 5.15** in particular display longitudinal cracking along the bars within the splice zone, which is indicative of a bond-splitting failure. Appendix A contains the photographs of the nine beam splice specimens after failure.

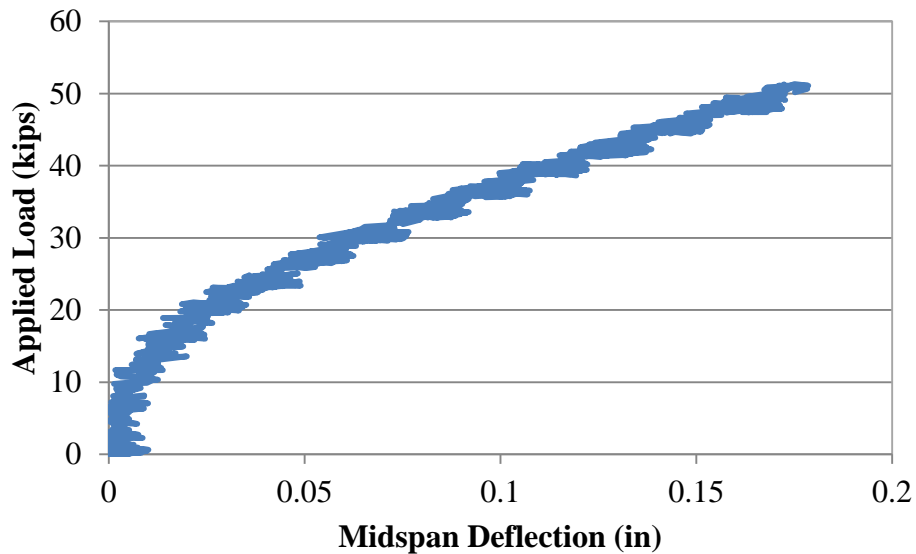


Figure 5.11 – Typical load vs. deflection plot

Conversion: 1 in. = 25.4 mm

1 kip = 4.45 kN

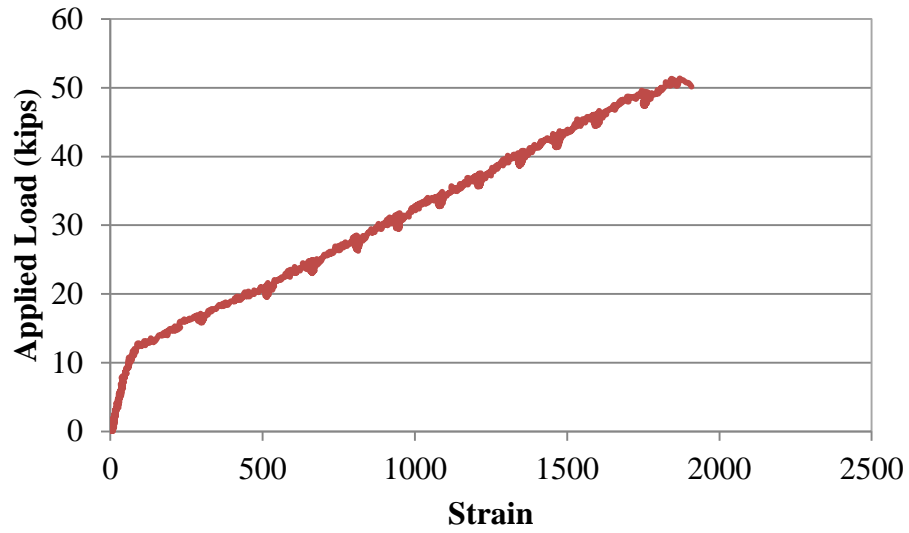


Figure 5.12 – Typical load vs. strain plot
Conversion: 1 kip = 4.45 kN



Figure 5.13 – Cracked length of HVFA-70HBB2

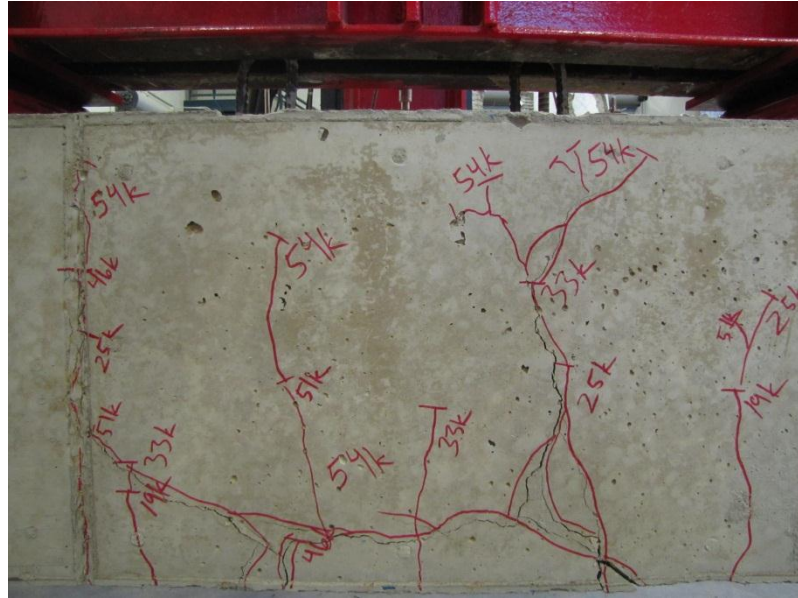


Figure 5.14 – Failed splice region of HVFA-70HBB2



Figure 5.15 – Bottom of splice region of HVFA-70HBB2

5.3. REINFORCING BAR DIRECT TENSION TEST

A tension test was performed on the #6 (#19) longitudinal reinforcing bars used in each beam specimen following ASTM E8-09, “Standard Test Methods for Tension Testing of Metallic Materials” (ASTM E9-09). Three 30 in. (762 mm) lengths of reinforcing bar were clamped at each end in a 200,000 lb. (890 kN) Tinius Olson testing machine and load was applied until the bar fractured. The strain and applied load were recorded during testing. The strain with a 0.5% offset was recorded and used to determine the yield strength of each bar. The modulus of elasticity was also determined for each bar. The average yield stress of the test was used as a comparison tool to check that the reinforcing bars within the splice region of each beam specimen did not reach yield. **Table 5.5** displays the results of the tension test performed.

Table 5.5 – #6 (#19) reinforcing bar tension test results

Specimen	Yield Stress (ksi)	Average Yield Stress (ksi)	Initial Tangent Modulus (ksi)	Average Modulus (ksi)
1	81.1	81.1	33,130	30,310
2	81.3		26,510	
3	81.0		31,295	

Conversion: 1 ksi = 6.9 MPa

5.4. ANALYSIS OF RESULTS

5.4.1. Methodology. Direct comparison between test results is not possible due to the fact that the test day concrete strength varies for each mix. Therefore, normalization of the value of interest was completed to facilitate direct comparison of test results. Two separate normalization formulas were used in this study. The first normalization formula

is based on the development length equations in ACI 318-08 (ACI 318-08, 2008) and AASHTO LRFD-07 (AASHTO, 2007), shown as **Eq. 5.1** and **5.2**, respectively. Both equations express the development length of a reinforcing bar in tension as a function of the inverse square root of the compressive strength. Therefore, the first normalization of the test results was based on multiplying values by the square root of the ratio of the specified design strength and the test day compressive strength, shown in **Eq. 5.3**.

$$l_d = \left(\frac{3}{40} \frac{f_y}{\lambda \sqrt{f'_c}} \frac{\Psi_t \Psi_e \Psi_s}{\left(\frac{c_b + K_{tr}}{d_b} \right)} \right) d_b \quad (5.1)$$

Where l_d is the development length, f_y is the specified yield strength of reinforcement, λ is the lightweight concrete modification factor, f'_c is the specified compressive strength of concrete, Ψ_t is the reinforcement location modification factor, Ψ_e is the reinforcement coating modification factor, Ψ_s is the reinforcement size modification factor, c_b is the smaller of the distance from center of a bar to nearest concrete surface or one-half the center-to-center spacing of bars being developed, K_{tr} is the transverse reinforcement index, and d_b is the nominal diameter of reinforcing bar.

$$l_{db} = \frac{1.25 A_b f_y}{\sqrt{f'_c}} \geq 0.4 d_b f_y \quad (5.2)$$

Where l_{db} is the tension development length, f_y is the specified yield strength of reinforcement, A_b is the area of reinforcing bar, f'_c is the specified compressive strength of concrete, and d_b is the reinforcing bar diameter.

$$\text{Normalized Load} = \text{Failure load} \sqrt{\frac{\text{Design strength}}{\text{Strength at testing}}} \quad (5.3)$$

The second normalization formula is based on the development length equation in ACI 408R-04 (2003), as shown in **Eq. 5.4**. The development length of a reinforcing bar in tension in this equation is a function of the inverse fourth root of the compressive strength. Therefore, the normalization of the test results was based on the fourth root of the ratio of the specified design strength and the test day compressive strength, as shown in **Eq. 5.5**.

$$l_d = \left(\frac{\left(\frac{f_y}{f_c^{1/4}} - 1970 \omega \right) \alpha \beta \lambda}{62 \left(\frac{c + K_{tr}}{d_b} \right)} \right) d_b \quad (5.4)$$

Where l_d is the development length, f_y is the specified yield strength of reinforcement, λ is the lightweight concrete modification factor, f_c is the specified compressive strength of concrete, α is the reinforcement location modification factor, β is the reinforcement coating modification factor, ω is equal to $0.1 (c_{\max}/c_{\min}) + 0.9 \leq 1.25$, c is the spacing or cover dimension, d_b is the nominal diameter of reinforcing bar, and K_{tr} is the transverse reinforcement index.

$$\text{Normalized Load} = \text{Failure load} \left(\frac{\text{Design strength}}{\text{Strength at testing}} \right)^{1/4} \quad (5.5)$$

The design strength for the HVFA concrete test program was 4,000 psi (27.6 MPa) and the strengths at testing for each mix design can be seen in **Table 5.6**.

Table 5.6 – Test day compressive strengths for test specimens

	Test Day Strength (psi)				
	Cylinder 1	Cylinder 2	Cylinder 3	Average	COV (%)
HVFA-C	4560	4390	4480	4475	1.9
HVFA-70H	3300	3480	3560	3450	3.8
HVFA-70L	3530	3320	3415	3420	3.1

Conversion: 1 psi = 6.9 kPa

5.4.2. Analysis and Interpretation – Direct Pull-out Test Results. Table 5.7

contains the peak load, concrete strength at time of testing, and normalized peak load for each specimen. **Figure 5.16** is a plot of the square root normalized peak load for each of the mix designs and bar sizes. The error bars indicate the range of test data collected. For the #4 (#13), all three mix designs performed at essentially the same level. The HVFA-70H normalized peak load average was 131 lb. (0.6 kN) lower, and the HVFA-70L normalized peak load average was 286 lb. (1.3 kN) higher than that of the control, which represents differences of 1.4 and 3%, respectively. The closeness of these results indicates that both fly ash mix designs have the same level of bond strength as the control for #4 (#13) reinforcing bars, particularly given the expected variation in results. Slightly more variability occurred for the #6 (#19) bars. The HVFA-70H and HVFA-70L normalized peak load averages were 2,645 lb. (11.8 kN) and 2,321 lb. (10.3 kN) higher than that of the control, representing differences of 11.3 and 9.9%, respectively. However, paired t-tests indicate that there is no statistically significant difference

between the results for each mix design, indicating that the HVFA concrete has essentially the same bond strength as conventional concrete.

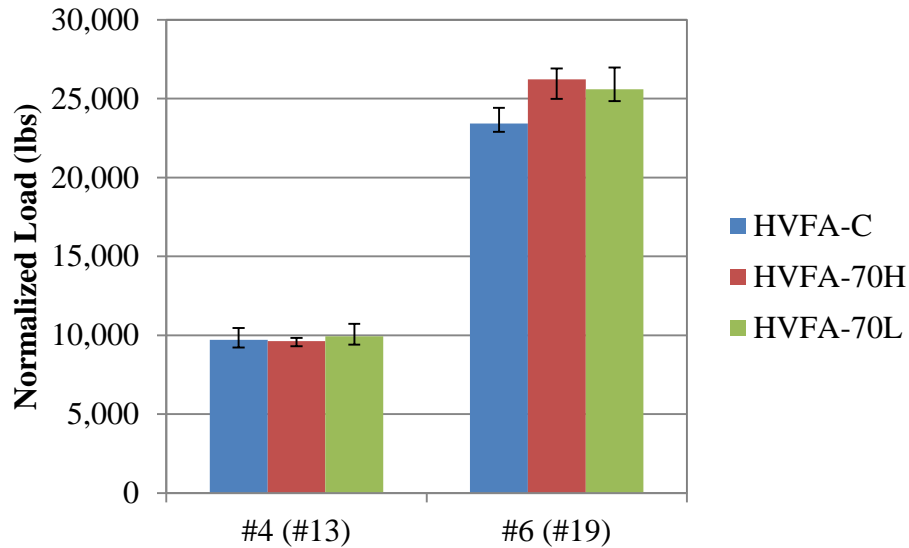


Figure 5.16 – Plot of normalized average peak load for each HVFA concrete mix design
Conversion: 1 lb. = 4.45 N

Figure 5.17 displays a representative normalized load vs. slip plot of the #4 (#13) pull-out specimens, and **Figure 5.18** displays the same plot for the #6 (#19) pull-out specimens. The plots indicate that bar slip occurred around the same load for each test specimen. More importantly, the overall behavior was very similar between all three mix designs. This behavior, combined with a forensic investigation of the failed specimens, indicates that the concrete surrounding the bar crushed around the same load for both fly ash mixes and the control mix.

Table 5.7 – Normalized HVFA concrete pull-out test results

Mix	Bar Size	Specimen	Peak Load (lb.)	Concrete Compressive Strength (psi)	Normalized Load (lb.)				COV (%)
					Square Root Adjustment	Fourth Root Adjustment	Average of Square Root Adjustment	Average of Fourth Root Adjustment	
HVFA-C	#4 (#13)	4PO1	10,002	4,476	9,455	9,725	9,708	9,985	6.8
		4PO2	11,058		10,453	10,752			
		4PO3	9,749		9,216	9,479			
	#6 (#19)	6PO1	24,289		22,961	23,616	23,429	24,097	
		6PO2	24,234		22,909	23,562			
		6PO3	25,829		24,417	25,113			
HVFA-70H	#4 (#13)	4PO1	8,604	3,464	9,246	8,919	9,577	9,239	3.0
		4PO2	9,091		9,769	9,424			
		4PO3	9,042		9,716	9,373			
	#6 (#19)	6PO1	24,770		26,617	25,677	26,074	25,153	
		6PO2	24,902		26,759	25,814			
		6PO3	23,120		24,845	23,967			
HVFA-70L	#4 (#13)	4PO1	9,989	3,422	10,799	10,386	9,994	9,611	7.1
		4PO2	8,750		9,460	9,098			
		4PO3	8,992		9,722	9,350			
	#6 (#19)	6PO1	23,120		24,997	24,040	25,750	24,765	
		6PO2	25,108		27,146	26,107			
		6PO3	23,222		25,107	24,146			

Conversion: 1 in. = 25.4 mm

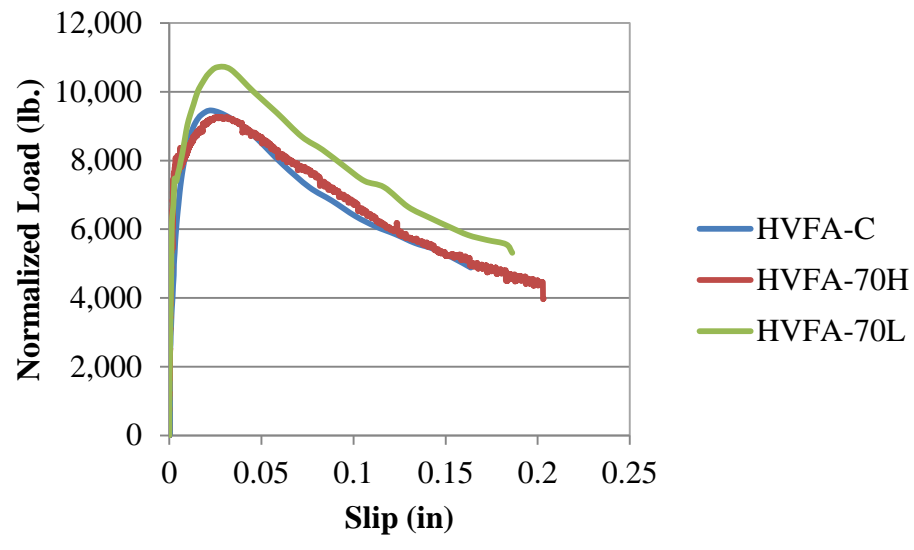


Figure 5.17 – Normalized load vs. slip plot for #4 (#13) reinforcing bars
Conversion: 1 in. = 25.4 mm
1 lb. = 4.45 N

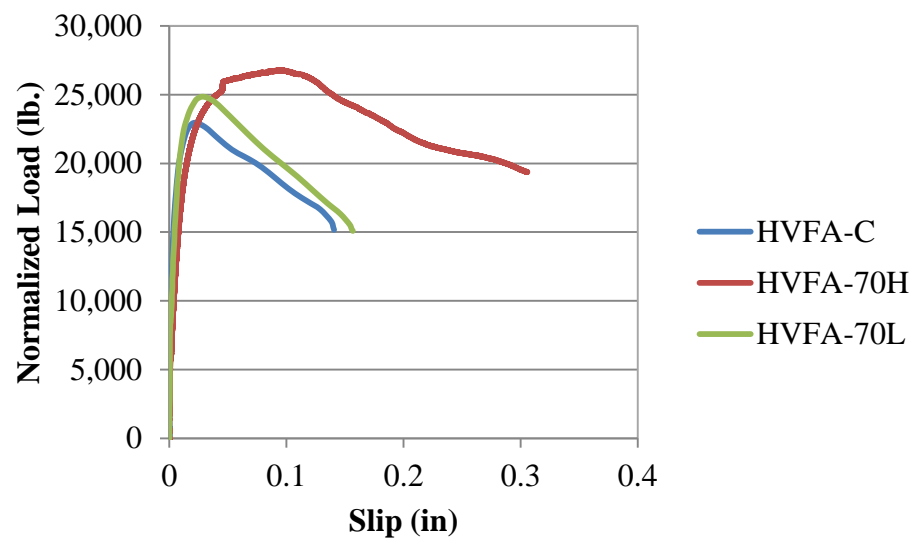


Figure 5.18 – Load vs. slip plot for #6 (#19) reinforcing bars
Conversion: 1 in. = 25.4 mm
1 lb. = 4.45 N

5.4.3. Analysis and Interpretation – Beam Splice Test Results. Table 5.8

contains the peak load, concrete strength at time of testing, and normalized peak load of each specimen tested. The square root normalized peak loads are plotted in **Figure 5.19**. **Table 5.9** contains the measured steel stress at failure, concrete strength at time of testing, and normalized measured steel stress at failure. The square root normalized steel stresses are shown plotted in **Figure 5.20**. The error bars indicate the range of test data collected. The normalized steel stresses were compared to the theoretical stress calculated using the moment-curvature program Response-2000 (Bentz, 2000) and are shown in **Table 5.10**. The moment at midspan of the specimen used when calculating the theoretical stress was a combination of both applied load moment and dead load moment. The applied load moment includes the weight of the spreader beams used to distribute the load from the actuators. The design concrete strength of 4,000 psi (27.6 MPa) was used when calculating the theoretical steel stress.

The data collected indicates that both fly ash mix designs exhibited improved bond performance compared to the control mix design. The average longitudinal bar stress for the HVFA-70H and HVFA-70L bottom splice beam specimens was 14.4 ksi (99 MPa) and 7.4 ksi (51 MPa) higher than that of the control bottom splice specimens, which represents a difference of 29 and 15%, respectively. The top splice beam specimens showed a similar trend, with the HVFA-70H and HVFA-70L bar stress being 22.1 ksi (152 MPa) and 10.5 ksi (72 MPa) higher than the control specimen, which represents a difference of 49 and 23%, respectively. The peak load data shows the same trend. These results indicate that the HVFA concrete mix designs have higher bond strength than that of the control mix design.

Table 5.8 – Normalized peak loads for each specimen

Mix	Specimen	Max Applied Load (kips)	Concrete Compressive Strength (psi)	Normalized Load (kips)			
				Square Root Adjustment	Fourth Root Adjustment	Average of Square Root Adjustment	Average of Fourth Root Adjustment
HVFA-C	BB1	53.3	4476	50.4	51.8	48.7	50.1
	BB2	49.7		47.0	48.3		
	TB	49.5		46.8	48.1	N/A	N/A
HVFA-70H	BB1	55.9	3464	60.1	57.9	60.2	58.1
	BB2	56.1		60.3	58.2		
	TB	60.2		64.7	62.4	N/A	N/A
HVFA-70L	BB1	55.2	3422	59.7	57.4	57.5	55.3
	BB2	51.1		55.2	53.1		
	TB	55.1		59.6	57.3	N/A	N/A

Conversion: 1 kip = 4.45 kN

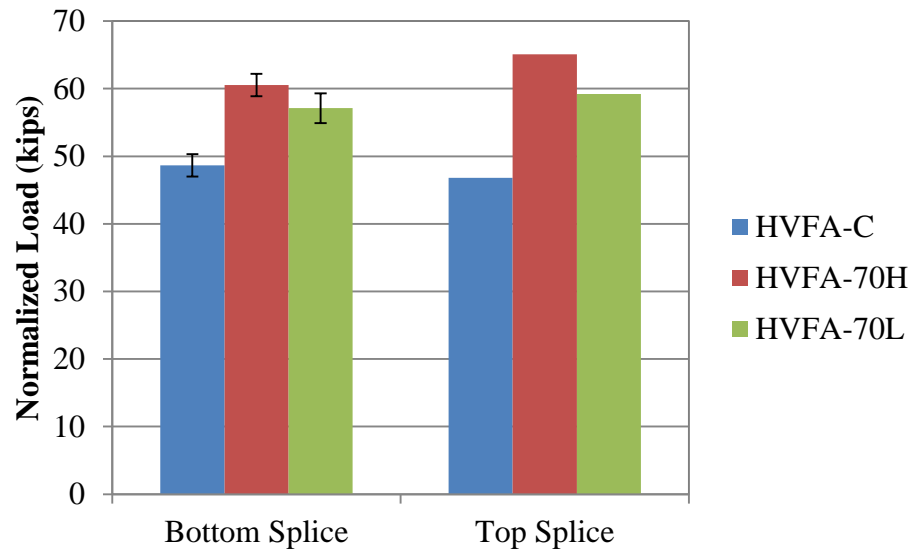


Figure 5.19 – Normalized peak load
Conversion: 1 kip = 4.45 kN

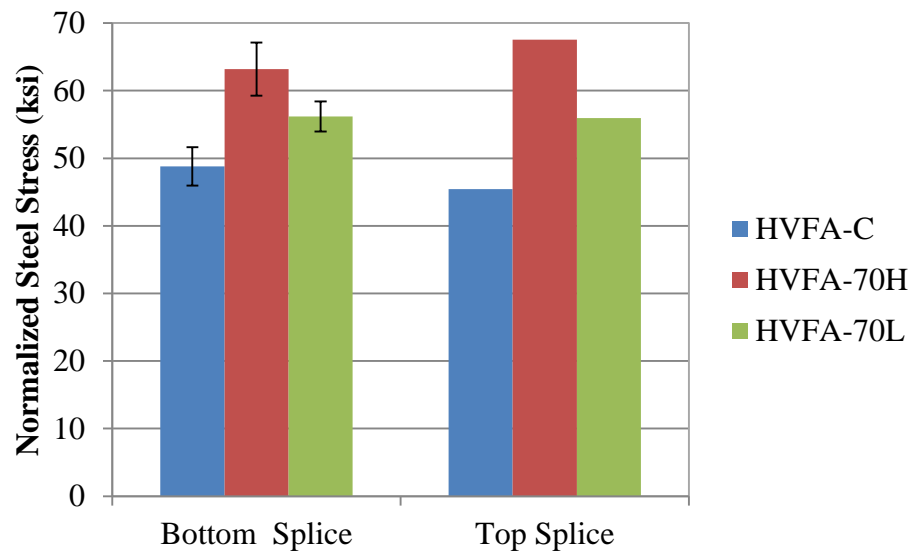


Figure 5.20 – Normalized steel stress at failure load
Conversion: 1 kip = 4.45 kN

Table 5.9 – Normalized steel stress at failure for each specimen

Mix	Specimen	Steel Stress Measured at Failure (ksi)	Concrete Compressive Strength (psi)	Normalized Steel Stress (ksi)	
				Square Root Adjustment	Fourth Root Adjustment
HVFA-C	BB1	54.6	4476	51.6	53.1
	BB2	48.6		46.0	47.3
	TB	48.1		45.4	46.7
HVFA-70H	BB1	62.4	3464	67.1	64.7
	BB2	55.1		59.2	57.2
	TB	62.8		67.5	65.1
HVFA-70L	BB1	54.0	3422	58.4	56.2
	BB2	49.9		53.9	51.9
	TB	51.7		55.9	53.8

Conversion: 1 ksi = 6.9 MPa

Table 5.10 – Normalized steel stress compared to theoretical steel stress at failure

Mix	Specimen	Normalized Steel Stress (ksi)		Calculated Stress at Failure Load (ksi)	Measured/Calculated Stress	
		Square Root Adjustment	Fourth Root Adjustment		Square Root Adjustment	Fourth Root Adjustment
HVFA-C	BB1	51.6	53.1	51.0	0.99	1.04
	BB2	46.0	47.3	47.6	1.04	0.99
	TB	45.4	46.7	47.5	1.05	0.98
HVFA-70H	BB1	67.1	64.7	53.4	0.80	1.21
	BB2	59.2	57.2	53.6	0.90	1.07
	TB	67.5	65.1	57.5	0.85	1.13
HVFA-70L	BB1	58.4	56.2	52.8	0.90	1.06
	BB2	53.9	51.9	49.0	0.91	1.06
	TB	55.9	53.8	52.7	0.94	1.02

Conversion: 1 ksi = 6.9 MPa

The difference in bond strength between the high and low cementitious material fly ash mix designs can be attributed to the difference in paste content of each mix. The higher paste content can facilitate consolidation of the concrete and allow for a more thorough coating of concrete around the perimeter of the reinforcing bar, thus increasing bonded area.

Normalized load vs. strain of the longitudinal reinforcing bar was also plotted for comparison. A typical plot of the average bottom splice strain for a specimen of each mix design is shown in **Figure 5.21**. As seen in the plot, all three specimens have two distinct linear sections. The first represents pre-flexural cracking behavior and the second represents post-flexural cracking behavior. The HVFA-70H specimen had a much lower cracking load than either mix. This was typical behavior of all HVFA-70H beam specimens. Most importantly, all load-strain plots indicated linear behavior up to failure. In other words, the reinforcing bars failed in bond, having never reached yield.

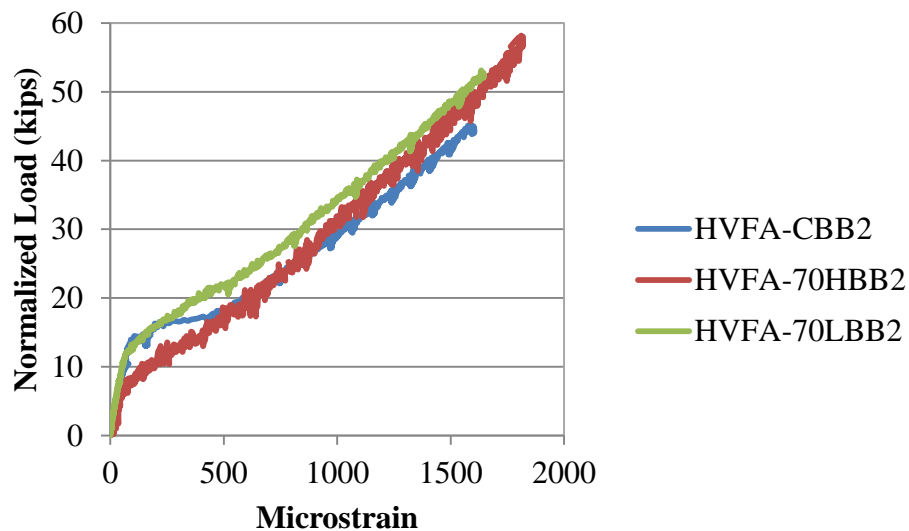


Figure 5.21 – Typical normalized load vs. strain plot
Conversion: 1 kip = 4.45 kN

5.5. FINDINGS AND CONCLUSIONS

Based on an analysis of the test results, the following conclusions are presented:

1. The average peak load for the #4 (#13), HVFA-70H and HVFA-70L pull-out specimens was 0.7% lower and 2.3% higher than that of the control, respectively. The average peak load for the #6 (#19), HVFA-70H and HVFA-70L pull-out specimens was 12% and 9.2% higher than that of the control, respectively. This data indicates that both HVFA mix designs have comparable bond strengths to the control mix design with #4 (#13) bars and higher bond strength with #6 (#19) bars. However, statistical analysis indicates that all three mix designs performed equally.
2. The average peak bar stress for the HVFA-70H and HVFA-70L bottom splice beam specimens was 29% and 15% higher than that of the control specimens, respectively. The peak bar stress for the HVFA-70H and HVFA-70L top splice beam specimens was 49% and 23% higher than that of the control specimens, respectively. This data indicates that both HVFA mix designs exhibited improved bond performance under realistic stress states than the control mix design.

6. FINDINGS, CONCLUSIONS, AND RECOMMENDATIONS

The main objective of this study was to determine the effect on bond performance of high-volume fly ash (HVFA) concrete. The HVFA concrete test program consisted of comparing the bond performance of two concrete mix designs with 70% cement replacement with Class C fly ash relative to a Missouri Department of Transportation (MoDOT) standard mix design at one strength level.

Two test methods were used for bond strength comparisons. The first was a direct pull-out test based on the RILEM 7-II-128 “RC6: Bond test for reinforcing steel. 1. Pull-out test” (RILEM, 1994). Although not directly related to the behavior of a reinforced concrete beam in flexure, the test does provide a realistic comparison of bond between types of concrete. The second test method consisted of a full-scale beam splice test specimen subjected to a four-point loading until failure of the splice. This test method is a non-ASTM test procedure that is generally accepted as the most realistic test method for both development and splice length.

This section contains the findings of both test programs, as well as conclusions based on these findings and recommendations for future research.

6.1. FINDINGS

6.1.1. Direct Pull-out Testing. A total of 18 direct pull-out test specimens were constructed for the HVFA concrete test program. There were six test specimens constructed for each of the HVFA concrete mix designs, as well as for the control mix design. Of the six specimens constructed for each mix design, three specimens contained

a #4 (#13) reinforcing bar and three specimens contained a #6 (#19) reinforcing bar. Each specimen was tested until failure. The average peak load for the #4 (#13), HVFA-70H and HVFA-70L pull-out specimens was 0.7% lower and 2.3% higher than that of the control, respectively. The average peak load for the #6 (#19), HVFA-70H and HVFA-70L pull-out specimens was 11.3% and 9.9% higher than that of the control, respectively.

6.1.2. Beam Splice Testing. A total of nine test specimens with 3#6 (#19) longitudinal reinforcing bars spliced at midspan were constructed for the HVFA concrete test program. There were three test specimens constructed for each of the two HVFA concrete mix designs to be evaluated, as well as for the control mix design. Of the three test specimens, two specimens were constructed with the spliced reinforcing bar located at the bottom of the beam cross section and one specimen was constructed with the splice at the top of the beam cross section to evaluate the top-bar effect. Each specimen was tested to bond failure. The average peak bar stress for the HVFA-70H and HVFA-70L bottom splice beam specimens was 29.5% and 15.2% higher than that of the control specimens, respectively. The peak bar stress for the HVFA-70H and HVFA-70L top splice beam specimens was 48.7% and 23.1% higher than that of the control specimens, respectively.

6.2. CONCLUSIONS

6.2.1. Direct Pull-out Testing. Analysis of the data indicates that both HVFA concrete mix designs have comparable bond strengths to the control mix design with #4 (#13) bars and higher bond strength with #6 (#19) bars. However, statistical analysis indicates that all three mix designs performed comparably.

6.2.2. Beam Splice Testing. Analysis of the data indicates that both HVFA concrete mix designs exhibited improved bond performance under realistic stress states than the control mix design. These findings, along with the findings from the direct pull-out tests, indicate that using greater than 50% replacement of cement with fly ash in concrete is feasible in terms of bond and development of reinforcing steel.

6.3. RECOMMENDATIONS

Future research in bond behavior of HVFA concrete is necessary due to the limited number of studies conducted on the subject. Much more research must be completed in order to create a more sizeable database that can eventually be used for comparison as well as for future ACI design code changes. Also important for design would be to explore whether or not certain ACI code distinctions, such as confinement, bar size, or bar coating factors, used for conventional concrete designs also apply to HVFA concrete, or if they need to be developed specifically for HVFA concrete. Below is a list of recommendations for testable variables related to HVFA concrete bond behavior:

- Perform tests with a larger variation in bar sizes based on ACI 318 code distinctions for bar size effect on development length
- Test pull-out specimens designed to fail by splitting rather than pull-out of the reinforcing bar
- Conduct direct tension on reinforcing bar embedded in HVFA concrete to determine development length and compare to the current ACI code provisions
- Perform studies with fly ash from different sources

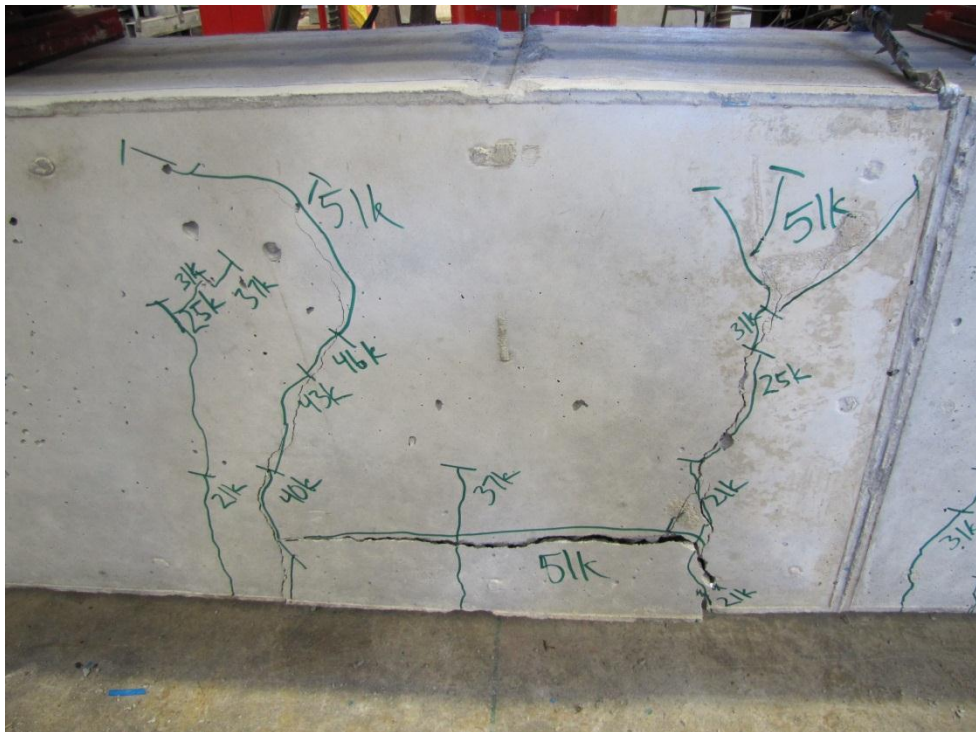
- Perform studies with aggregates form different sources
- Perform bond tests on more specimen types mentioned in ACI 408

APPENDIX A

HVFA TEST PROGRAM BEAM SPLICE FAILURE PHOTOGRAPHS



(a) Bottom view



(b) Side view

Figure A.1 – HVFA-CBB1



(a) Bottom View

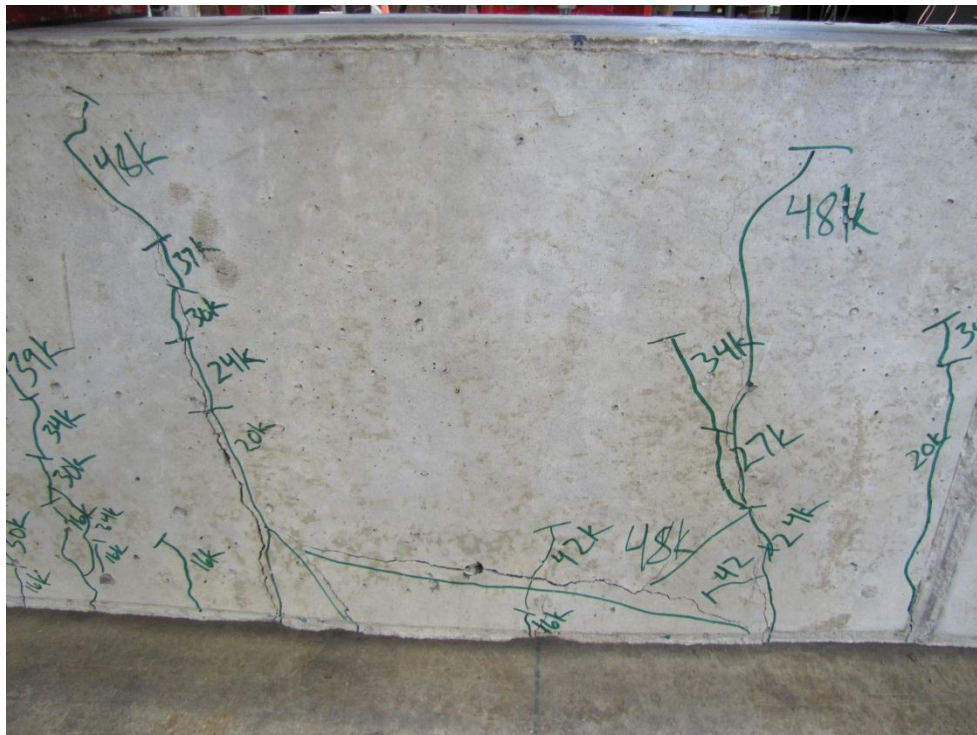


(b) Side View

Figure A.2 – HVFA-CBB2



(a) Bottom View



(b) Side View

Figure A.3 – HVFA-CTB



(a) Bottom View

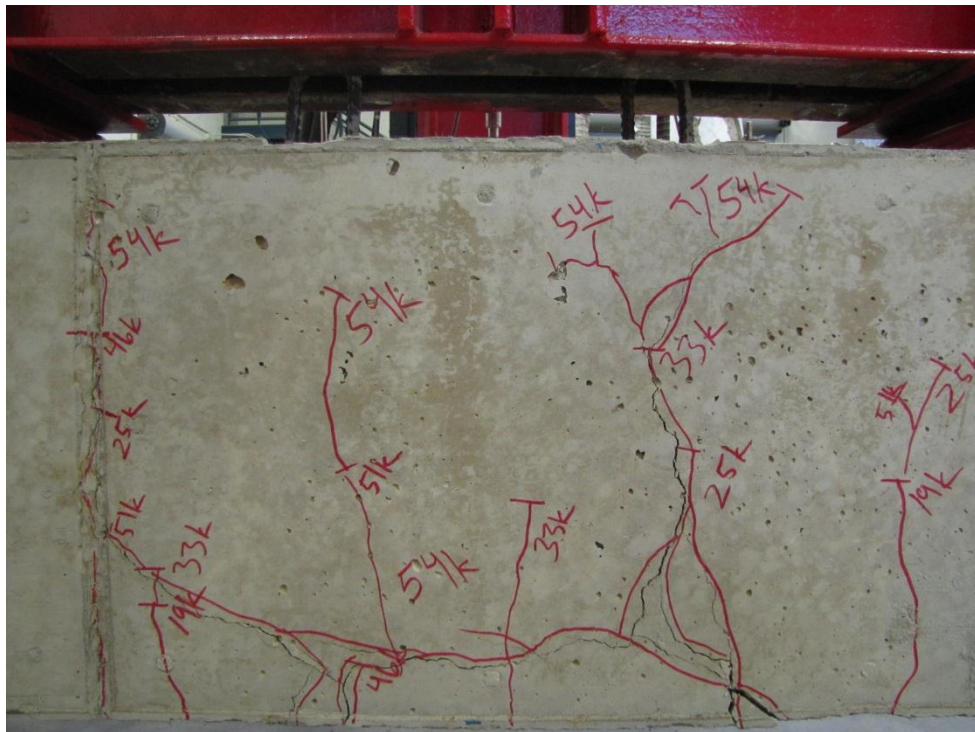


(b) Side View

Figure A.4 – HVFA-70HBB1



(a) Bottom View

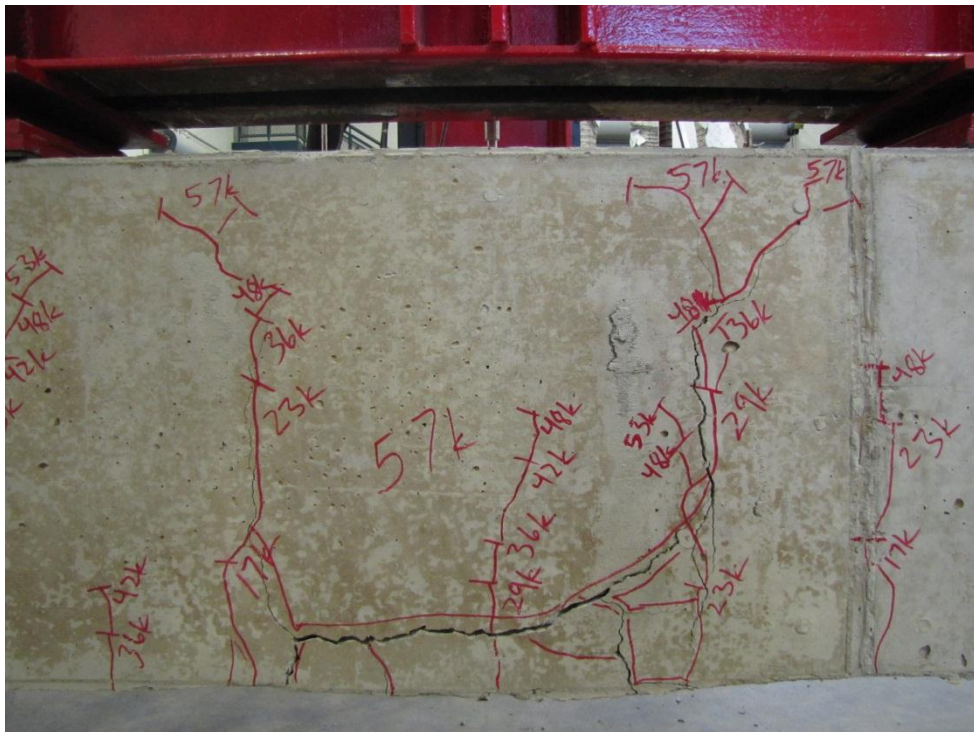


(b) Side View

Figure A.5 – HVFA-70HBB2



(a) Bottom View

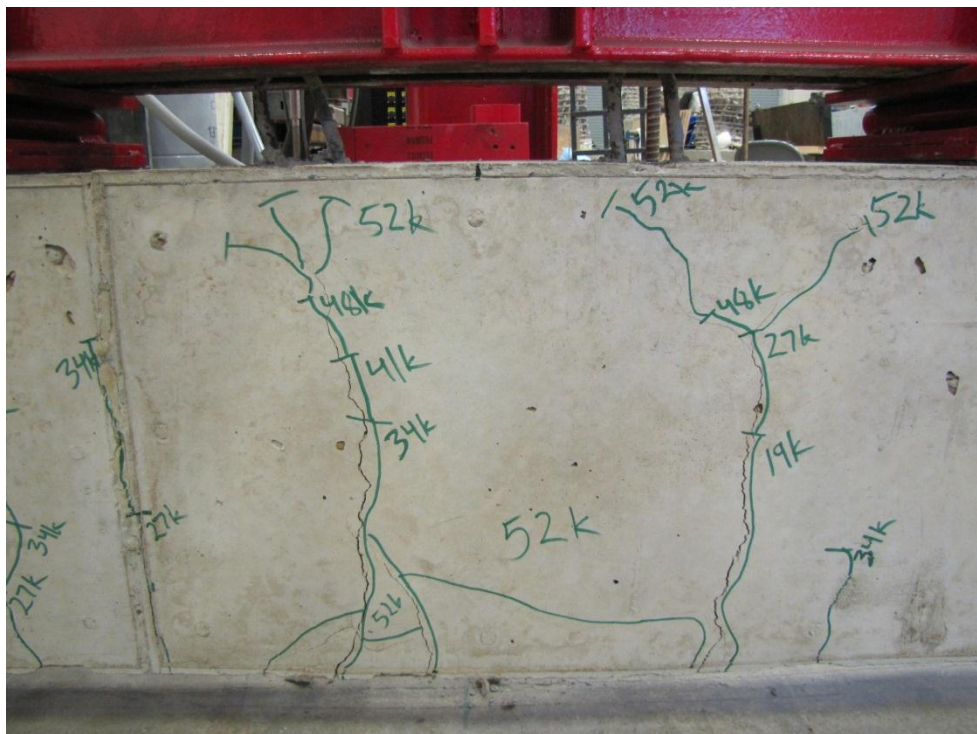


(b) Side View

Figure A.6 – HVFA-70HTB



(a) Bottom View

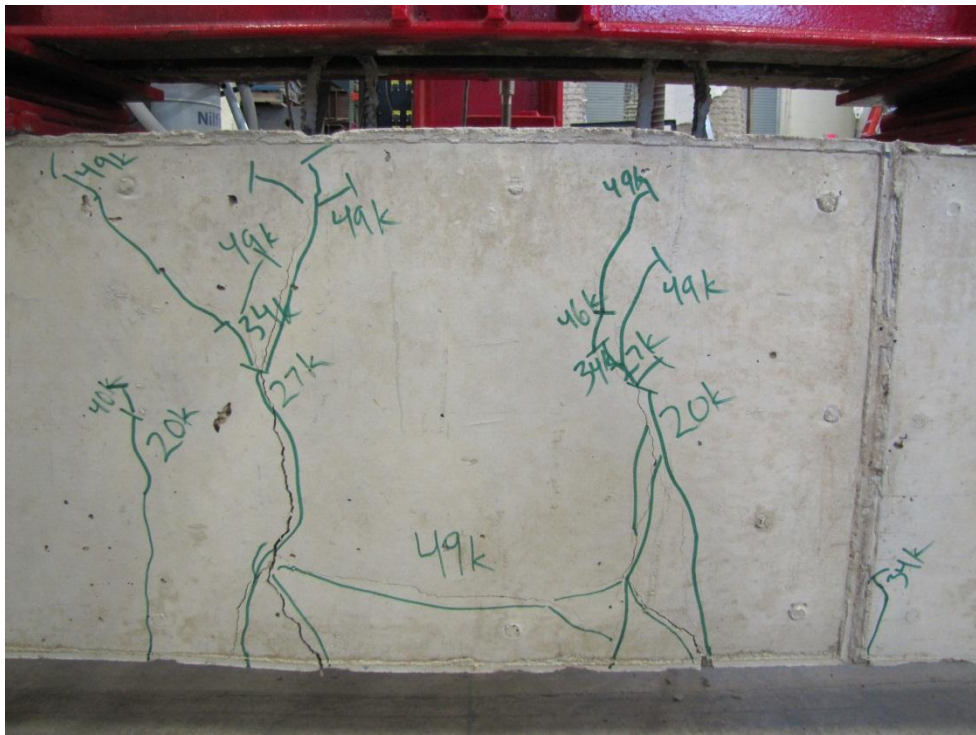


(b) Side View

Figure A.7 – HVFA-70LBB1



(a) Bottom View



(b) Side View

Figure A.8 – HVFA-70LBB2

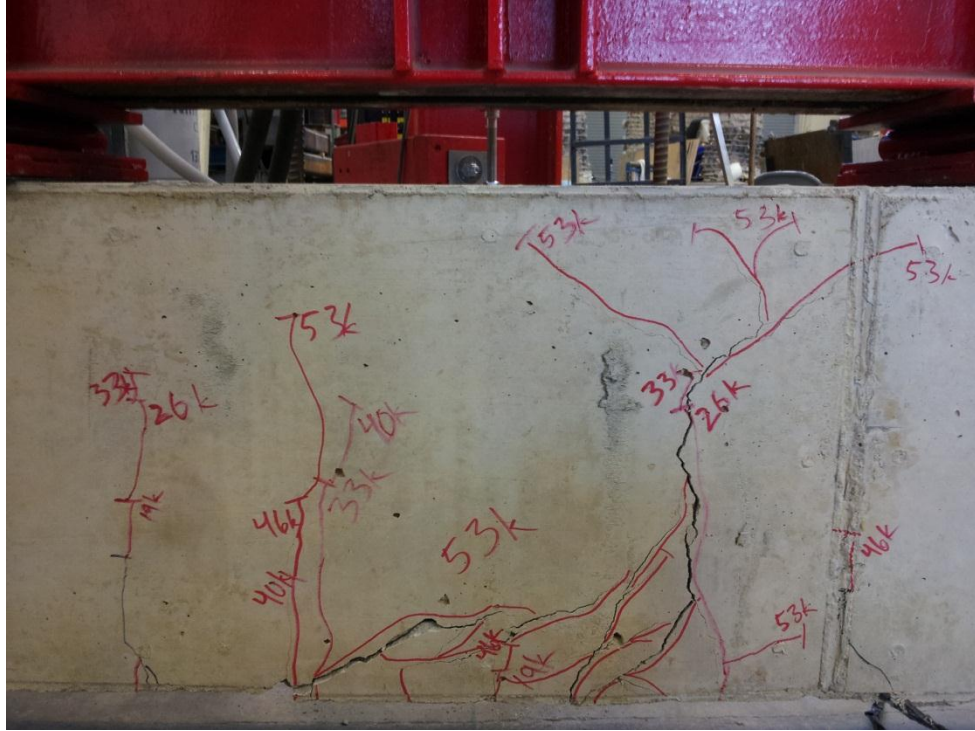


Figure A.9 – HVFA-70LTB side view

APPENDIX B

HVFA TEST PROGRAM TEST DATA PLOTS

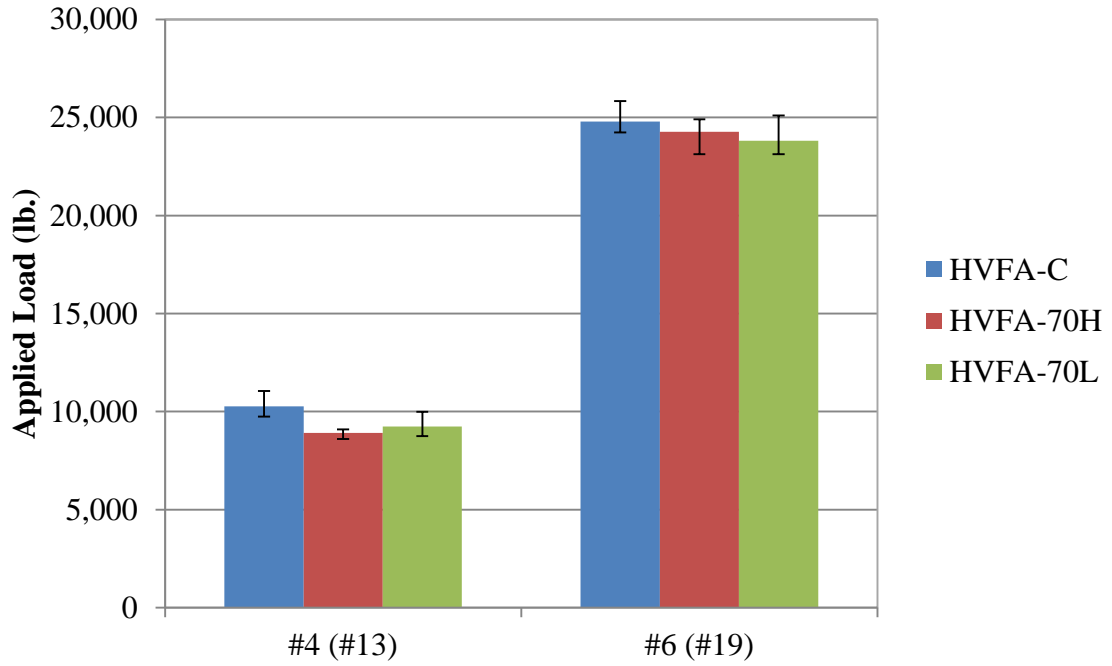


Figure B.1 – Direct pull-out applied load comparisons
 Conversion: 1 lb. = 4.45 N

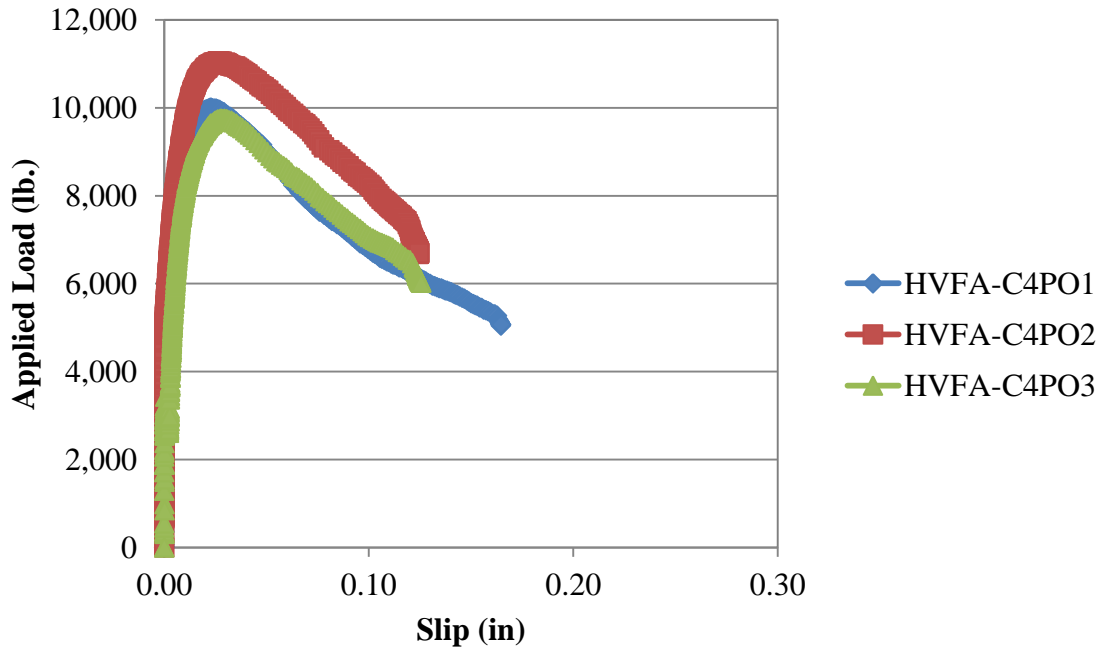


Figure B.3 – Applied load vs. slip plot for #4 (#13) HVFA-C
 Conversion: 1 in. = 25.4 mm
 1 lb. = 4.45 N

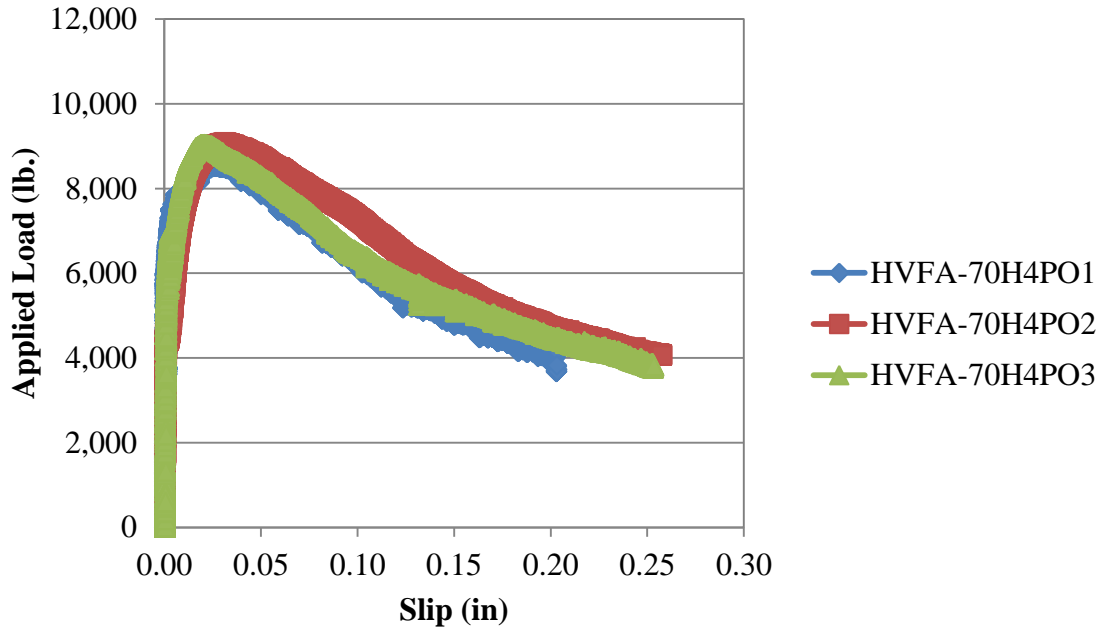


Figure B.4 – Applied load vs. slip plot for #4 (#13) HVFA-70H

Conversion: 1 in. = 25.4 mm

1 lb. = 4.45 N

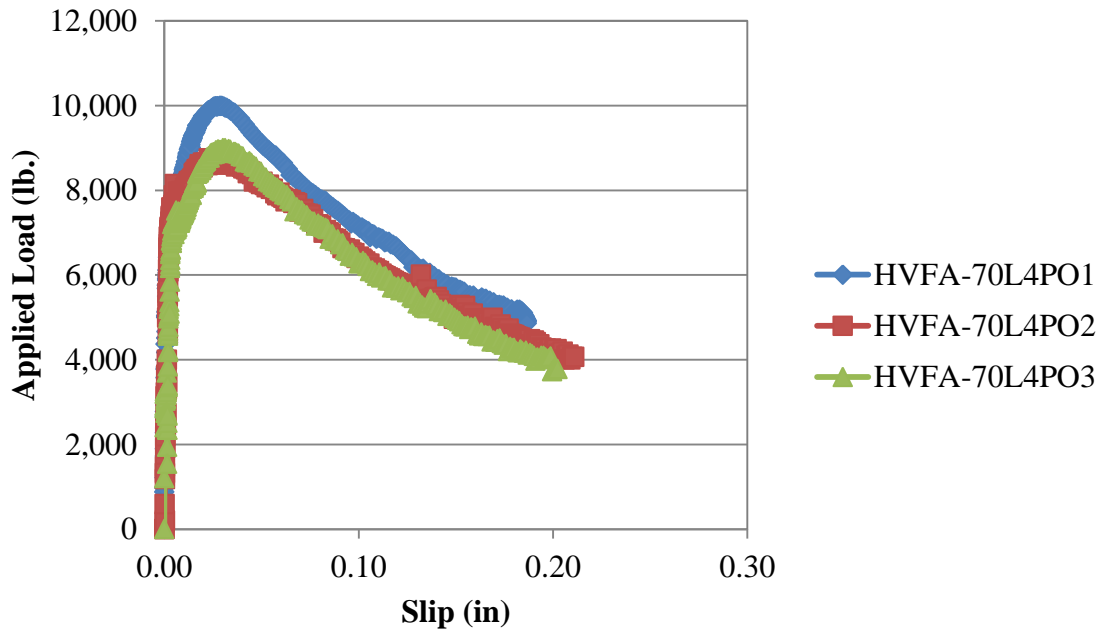


Figure B.5 – Applied load vs. slip plot for #4 (#13) HVFA-70L

Conversion: 1 in. = 25.4 mm

1 lb. = 4.45 N

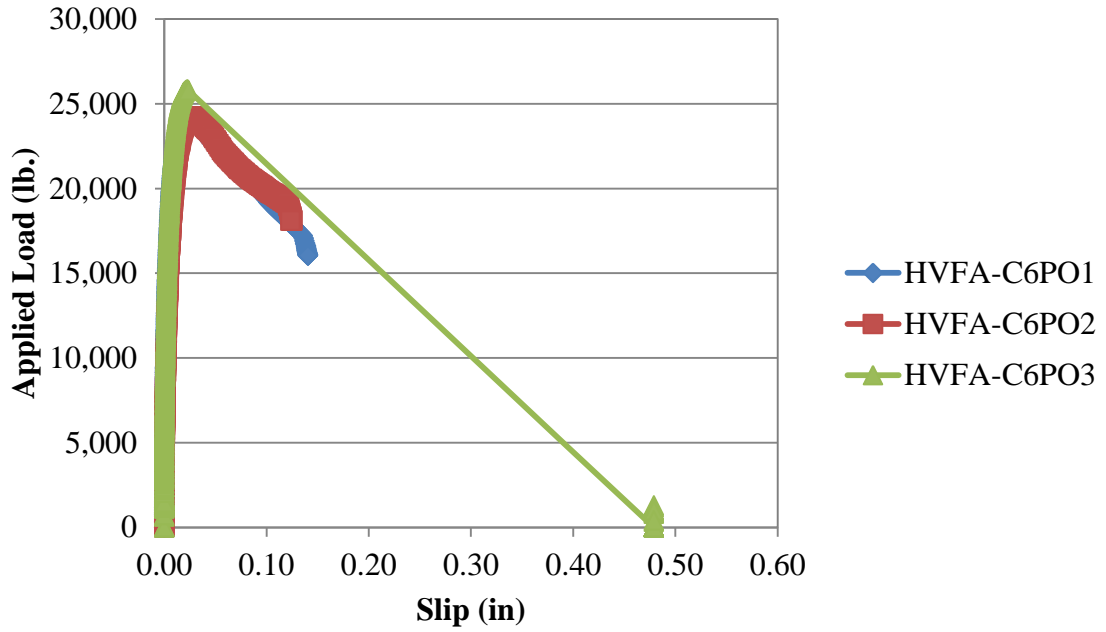


Figure B.6 – Applied load vs. slip plot for #6 (#19) HVFA-C

Conversion: 1 in. = 25.4 mm

1 lb. = 4.45 N

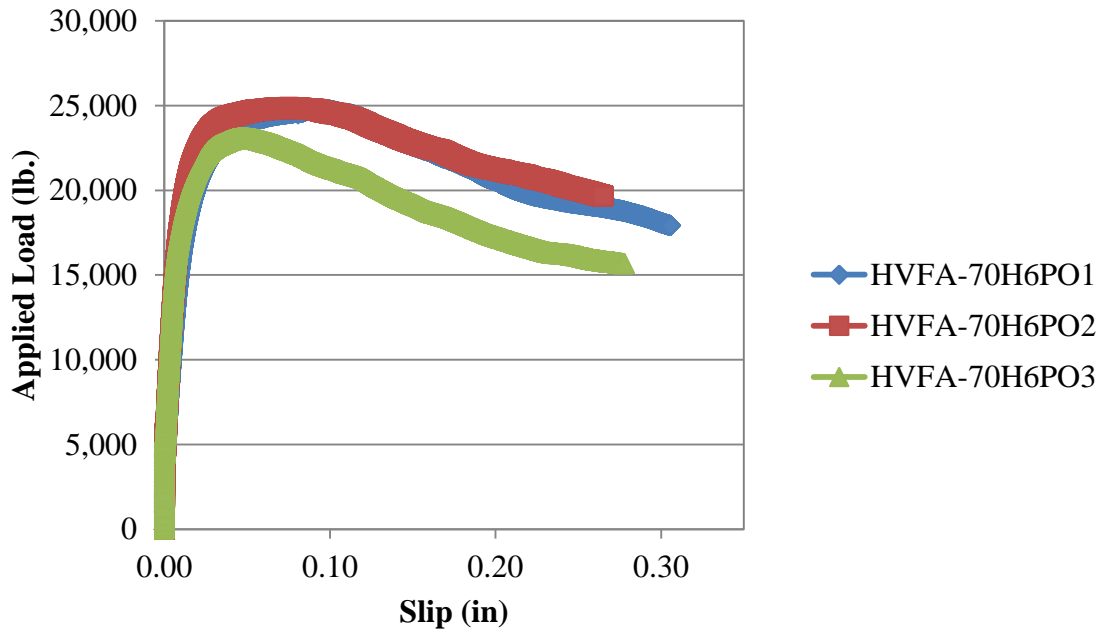


Figure B.7 – Applied load vs. slip plot for #6 (#19) HVFA-70H

Conversion: 1 in. = 25.4 mm

1 lb. = 4.45 N

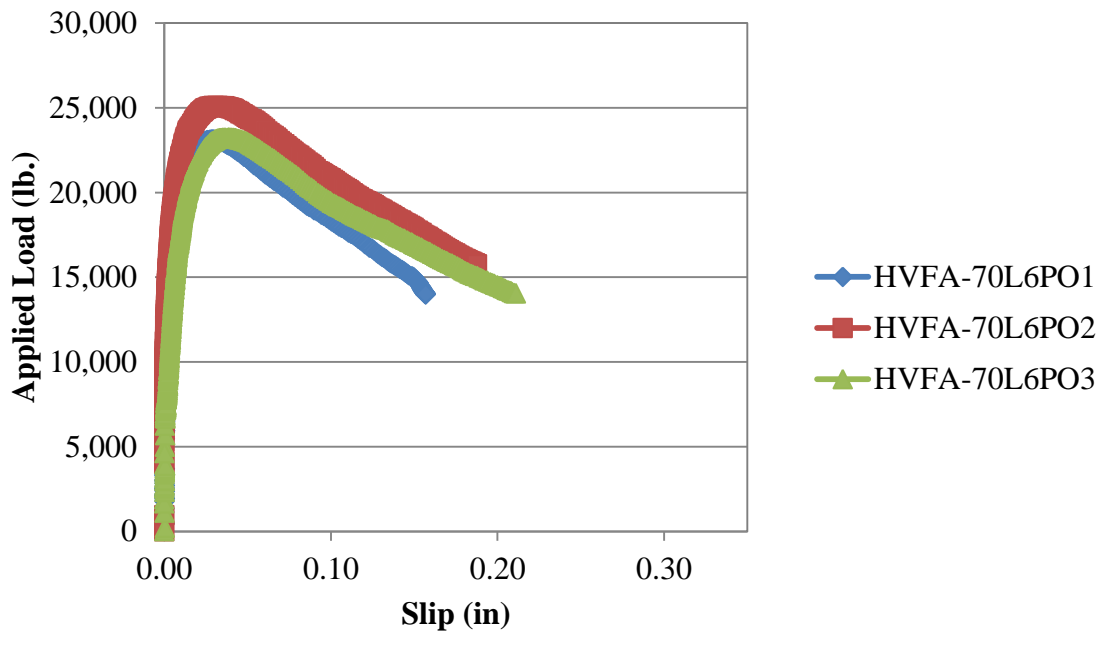


Figure B.8 – Applied load vs. slip plot for #6 (#19) HVFA-70L
Conversion: 1 in. = 25.4 mm
1 lb. = 4.45 N

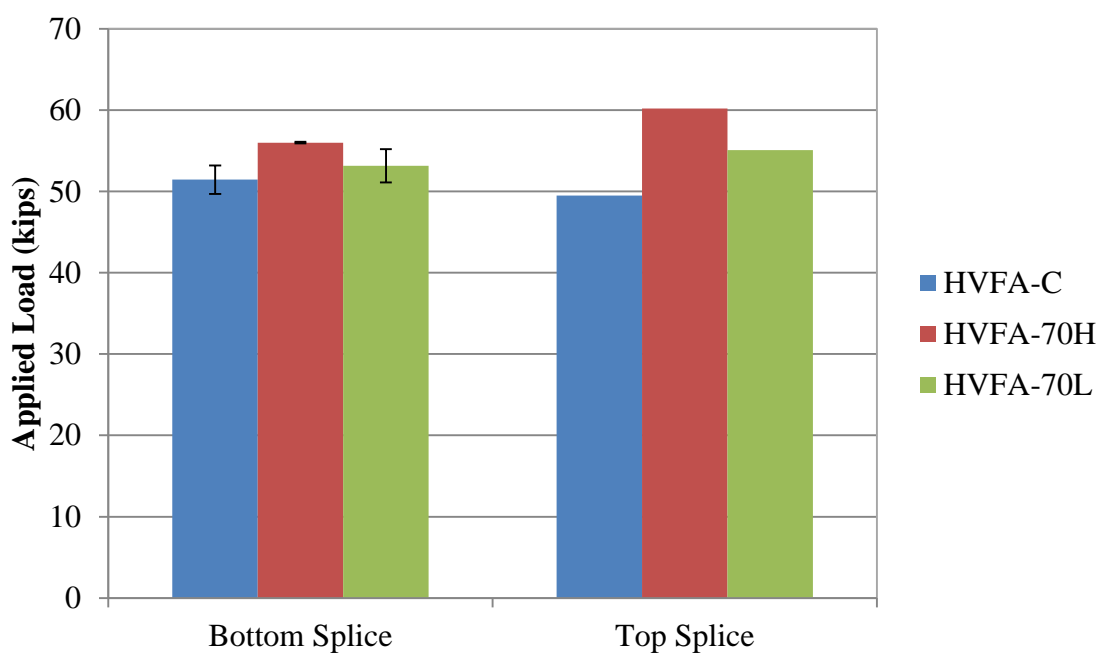


Figure B.11 – Beam splice applied load comparisons
Conversion: 1 kip = 4.45 kN

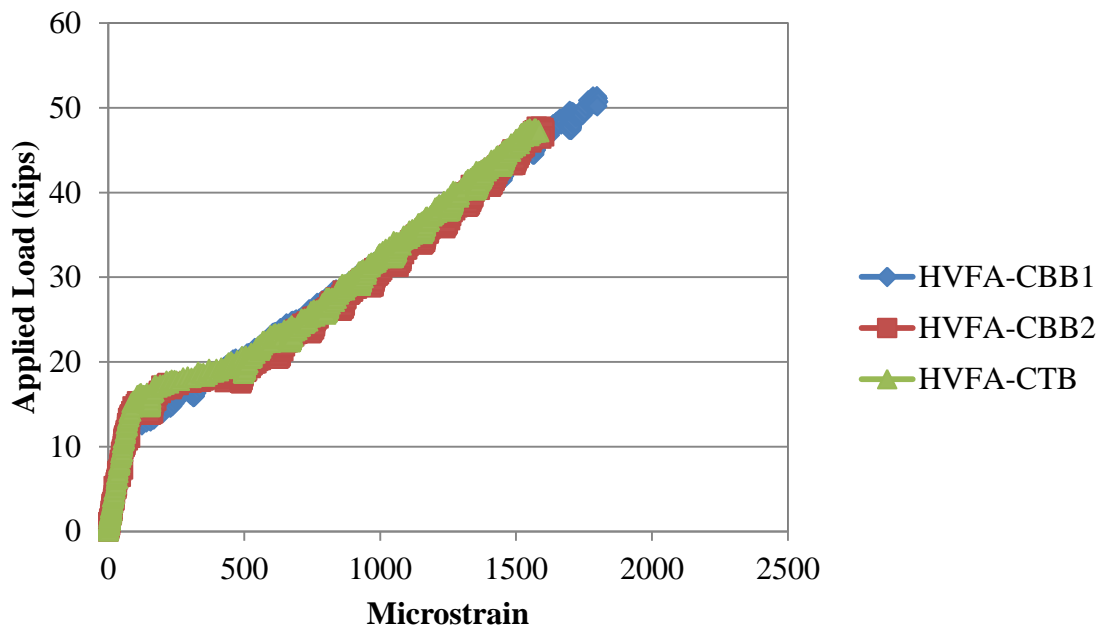


Figure B.13 – Applied load vs. strain (average of all gages per specimen) for HVFA-C
Conversion: 1 kip = 4.45 kN

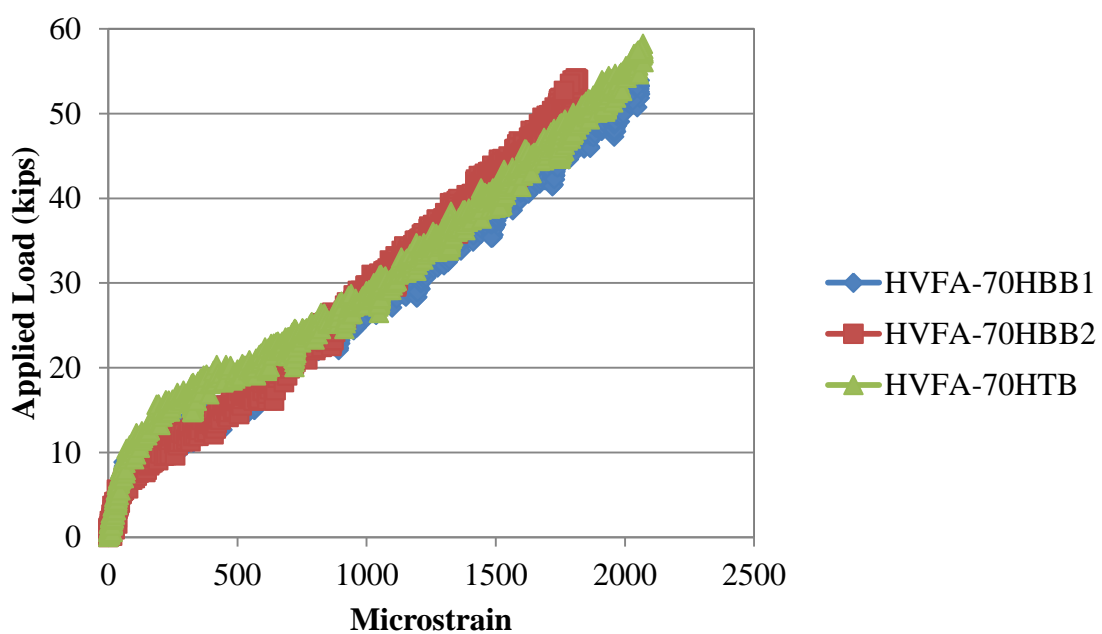


Figure B.14 – Applied load vs. strain (average of all gages per specimen) for HVFA-70H
Conversion: 1 kip = 4.45 kN

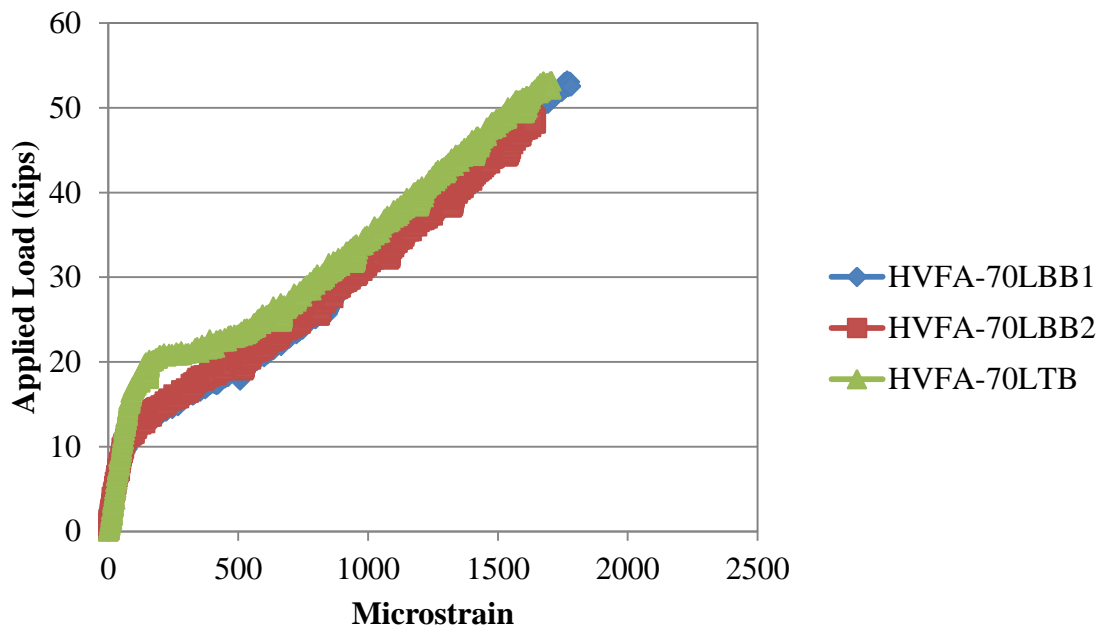


Figure B.15 – Applied load vs. strain (average of all gages per specimen) for HVFA-70L
Conversion: 1 kip = 4.45 kN

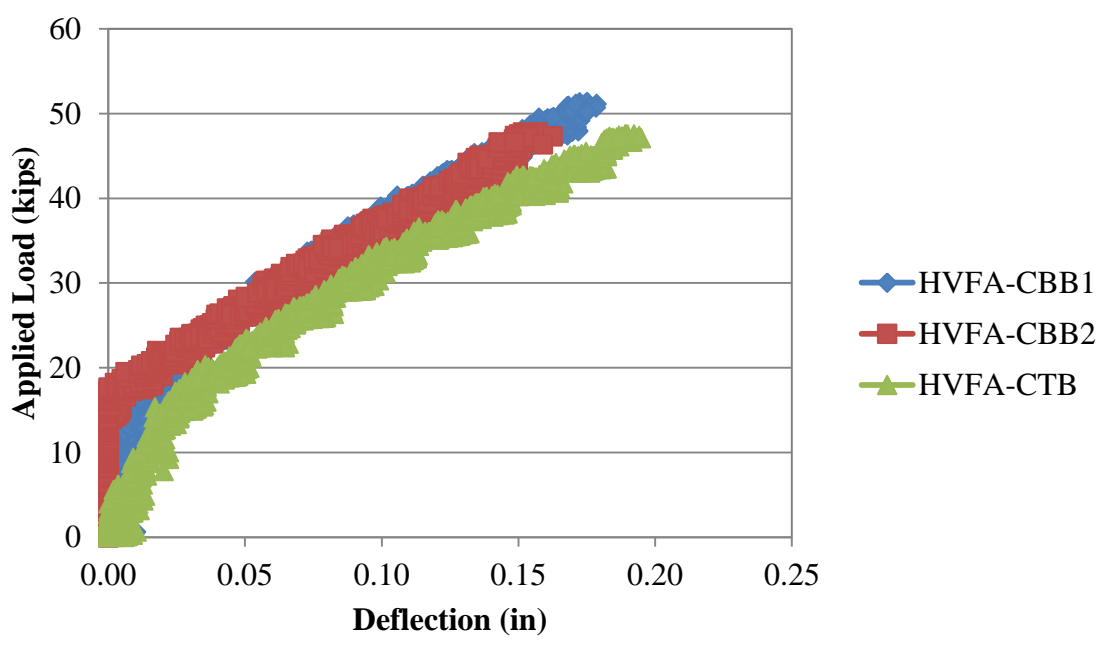


Figure B.16 – Applied load vs. displacement for HVFA-C
Conversion: 1 in. = 25.4 mm
1 kip. = 4.45 kN

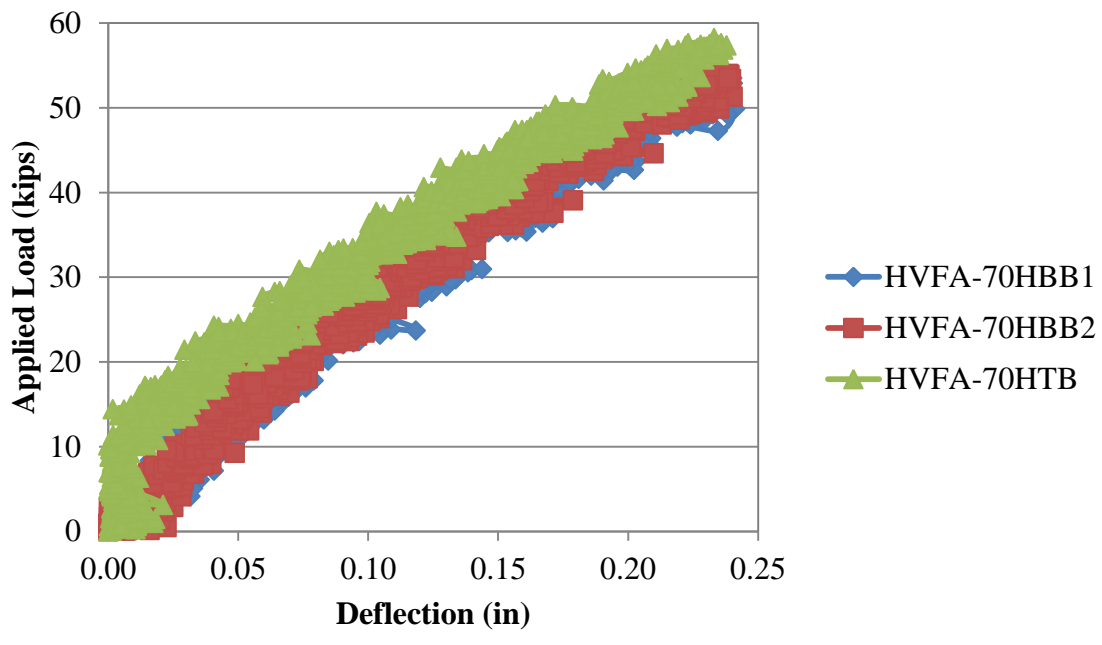


Figure B.17 – Applied load vs. displacement for HVFA-70H
Conversion: 1 in. = 25.4 mm
1 kip. = 4.45 kN

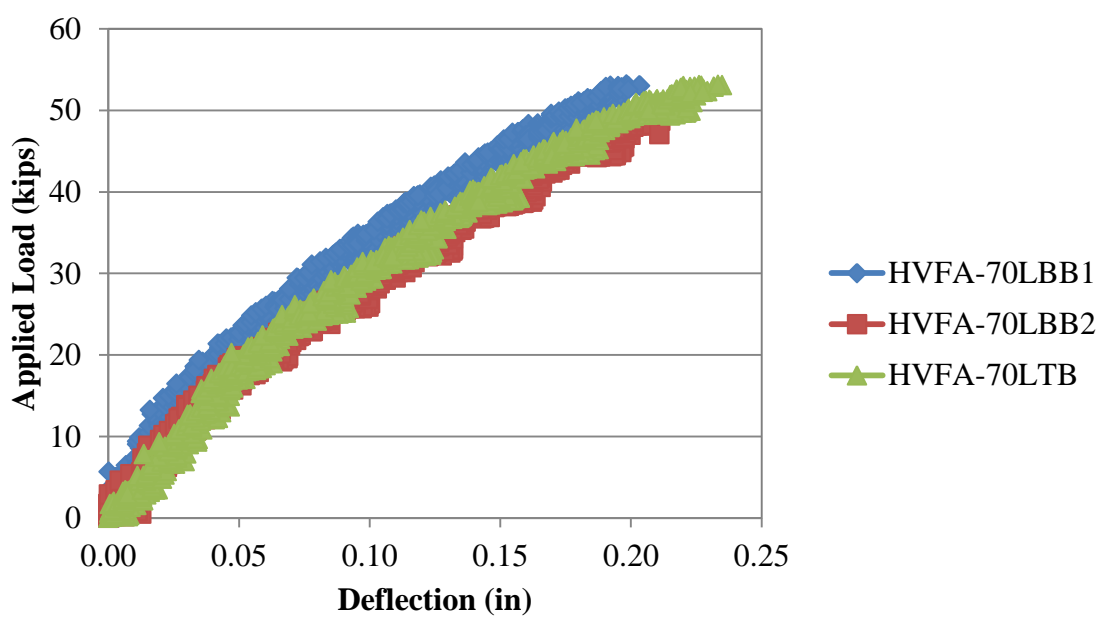


Figure B.18 – Applied load vs. displacement for HVFA-70L
Conversion: 1 in. = 25.4 mm
1 kip. = 4.45 kN

APPENDIX C

HVFA TEST PROGRAM STATISTICAL ANALYSIS

**Table C.1 – t-test for #4 (#13) HVFA-C and HVFA-70H
direct pull-out specimen average comparison**

	<i>Variable 1</i>	<i>Variable 2</i>
Mean	9708.257886	9635.442595
Variance	430834.9717	84064.43405
Observations	3	3
Pearson Correlation	0.576305254	
Hypothesized Mean Difference	0	
df	2	
t Stat	0.231990714	
P(T<=t) one-tail	0.419060699	
t Critical one-tail	2.91998558	
P(T<=t) two-tail	0.838121398	
t Critical two-tail	4.30265273	

**Table C.2 – t-test for #4 (#13) HVFA-C and HVFA-70L
direct pull-out specimen average comparison**

	<i>Variable 1</i>	<i>Variable 2</i>
Mean	9708.257886	9932.861212
Variance	430834.9717	497843.3526
Observations	3	3
	-	
Pearson Correlation	0.497953779	
Hypothesized Mean Difference	0	
df	2	
	-	
t Stat	0.329976631	
P(T<=t) one-tail	0.386387326	
t Critical one-tail	2.91998558	
P(T<=t) two-tail	0.772774651	
t Critical two-tail	4.30265273	

**Table C.3 – t-test for #6 (#19) HVFA-C and HVFA-70H
direct pull-out specimen average comparison**

	<i>Variable 1</i>	<i>Variable 2</i>
Mean	23429.14052	26233.26766
Variance	732596.0679	1151632.636
Observations	3	3
	-	
Pearson Correlation	0.999346127	
Hypothesized Mean Difference	0	
df	2	
	-	
t Stat	2.518156716	
P(T<=t) one-tail	0.064045916	
t Critical one-tail	2.91998558	
P(T<=t) two-tail	0.128091832	
t Critical two-tail	4.30265273	

**Table C.4 – t-test for #6 (#19) HVFA-C and HVFA-70L
direct pull-out specimen average comparison**

	<i>Variable 1</i>	<i>Variable 2</i>
Mean	23429.14052	26233.26766
Variance	732596.0679	1151632.636
Observations	3	3
	-	
Pearson Correlation	0.999346127	
Hypothesized Mean Difference	0	
df	2	
	-	
t Stat	2.518156716	
P(T<=t) one-tail	0.064045916	
t Critical one-tail	2.91998558	
P(T<=t) two-tail	0.128091832	
t Critical two-tail	4.30265273	

Table C.5 – t-test for HVFA-C and HVFA-70H beam splice average comparison

	<i>Variable 1</i>	<i>Variable 2</i>
Mean	47.68025213	64.6223856
Variance	11.79358493	21.70748414
Observations	3	3
Pearson Correlation	0.392158818	
Hypothesized Mean Difference	0	
df	2	
	-	
t Stat	6.410891402	
P(T<=t) one-tail	0.011738856	
t Critical one-tail	2.91998558	
P(T<=t) two-tail	0.023477711	
t Critical two-tail	4.30265273	

Table C.6 – t-test for HVFA-C and HVFA-70L beam splice average comparison

	<i>Variable 1</i>	<i>Variable 2</i>
Mean	47.68025213	56.09310113
Variance	11.79358493	4.983445281
Observations	3	3
Pearson Correlation	0.85801692	
Hypothesized Mean Difference	0	
df	2	
	-	
t Stat	7.657183005	
P(T<=t) one-tail	0.008315558	
t Critical one-tail	2.91998558	
P(T<=t) two-tail	0.016631115	
t Critical two-tail	4.30265273	

BIBLIOGRAPHY

- AASHTO (2007). AASHTO LRFD Bridge Design Specification. Fourth Edition, Washington, D.C.
- ACI 318 (2008). Building Code Requirements for Structural Concrete (ACI 318-08) and Commentary. American Concrete Institute, Farmington Hills, MI.
- ACI 408R (2003). Bond and Development of Straight Reinforcing Bars in Tension. American Concrete Institute, Farmington Hills, MI
- ASTM C 39 (2011). Standard Test Method for Compressive Strength of Cylindrical Concrete Specimens. *American Society for Testing and Materials*. West Conshohocken, PA.
- ASTM C 78 (2010). Standard Test Method for Flexural Strength of Concrete (Using Simple Beam with Third-Point Loading). *American Society for Testing and Materials*. West Conshohocken, PA.
- ASTM C 138 (2010). Standard Test Method for Density (Unit Weight), Yield, and Air Content (Gravimetric) of Concrete. *American Society for Testing and Materials*. West Conshohocken, PA.
- ASTM C 143 (2010). Standard Test Methods for Slump of Hydraulic Cement Concrete. *American Society for Testing and Materials*. West Conshohocken, PA.
- ASTM C 231 (2010). Standard Test Method for Air Content of Freshly Mixed Concrete by the Pressure Method. *American Society for Testing and Materials*. West Conshohocken, PA.
- ASTM C 496 (2011). Standard Test Method for Splitting Tensile Strength of Cylindrical Concrete Specimens. *American Society for Testing and Materials*. West Conshohocken, PA.
- ASTM C 618 (2012). Standard Specification for Coal Fly Ash and Raw or Calcined Natural Pozzolan for Use in Concrete. *American Society for Testing and Materials*. West Conshohocken, PA.
- ASTM E 8 (2009). Standard Test Methods for Tension Testing of Metallic Materials. *American Society for Testing and Materials*. West Conshohocken, PA.
- Bentz, E., Collins, M. (2000). Response-2000 Reinforced Concrete Sectional Analysis. Version 1.0.5. Toronto, Canada.

- Cross, D., Stephens, J., and Vollmer, J. (n.d.). "Structural Applications of 100 Percent Fly Ash Concrete." Montana State University, Bozeman, MT.
- Federal Highway Administration (2011). Coal Fly Ash – Material Description.
<<http://www.tfhr.gov/hnr20/recycle/waste/cfa51.htm>>
- Gopalakrishnan, S. (2005). "Demonstration of Utilising High Volume Fly Ash Based Concrete for Structural Applications." Structural Engineering Research Centre, Chennai India.
- Headwaters Resources (2011). Fly Ash for Concrete.
<<http://www.flyash.com/data/upimages/press/fly%20ash%20for%20concrete.pdf>>
- Marlay, K. (2011). "Hardened Concrete Properties and Durability Assessment of High-Volume Fly Ash Concrete." Thesis. Missouri S&T, Rolla, MO.
- Naik, T.R., Singh, S. S., Sivasundaram, V. (1989). "Concrete Compressives Strength, Shrinkage and Bond Strength As Affected by Addition of Fly Ash and Temperature." The University of Wisconsin – Milwaukee, Milwaukee, WI.
- RILEM 7-II-28. (1994). "Bond Test for Reinforcing Steel. 2. Pull-out test."
E & FN Spon, London.
- Volz, J., Myers, J. J. (2011) "Design and Evaluation of High-Volume Fly Ash Concrete Mixes." Missouri University of Science and Technology, Rolla, MO.
- Wight, J., MacGregor, J., "Reinforced Concrete Mechanics and Design." Fifth Edition. Upper Saddle River, NJ: Pearson Education, Inc., 2009. 360-406.
- Wolfe, M. (2011). "Bond Strength of High-Volume Fly Ash Concrete." M.S. Thesis, Missouri University of Science and Technology, Rolla, MO.